REPORT DOCUMENTATION PAGE

Form Approved OMB NO. 0704-0188

1. REPORT DATE (DD-MM-YYYY)	2. REPORT TYPE	3. DATES COVERED (From - To)
27-06-2014	Final Report	28-Mar-2012 - 28-Mar-2014

4. TITLE AND SUBTITLE
Development of a Biosensor Nanofluidic Platform for Integration With Terahertz Spectroscopic System

5a. CONTRACT NUMBER

5b. GRANT NUMBER
W911NF-12-C-0046

5c. PROGRAM ELEMENT NUMBER
606055

6. AUTHORS
T. Globus (PI), J. Ferrance, A. Moyer, M Levi, I. Sizov, B. Gelmont, H. Powell, A. Lichtenberger

5d. PROJECT NUMBER

5e. TASK NUMBER

5f. WORK UNIT NUMBER

7. PERFORMING ORGANIZATION NAMES AND ADDRESSES
Vibratess
2020 Avon Ct., Suite 43

Charlottesville, VA 22902 -8734

8. PERFORMING ORGANIZATION REPORT NUMBER

9. SPONSORING/MONITORING AGENCY NAME(S) AND ADDRESS (ES)
U.S. Army Research Office
P.O. Box 12211
Research Triangle Park, NC 27709-2211

10. SPONSOR/MONITOR'S ACRONYM(S)
ARO

11. SPONSOR/MONITOR'S REPORT NUMBER(S)
62043-EL-SB2.6

12. DISTRIBUTION AVAILIBILITY STATEMENT
Approved for Public Release; Distribution Unlimited

13. SUPPLEMENTARY NOTES
The views, opinions and/or findings contained in this report are those of the author(s) and should not contrued as an official Department of the Army position, policy or decision, unless so designated by other documentation.

14. ABSTRACT
Report delivered under topic #CBD 10-110, contract W911NF-12-C-0046.
The goal of this project is demonstration of a nanofluidic sensor platform effective for label-free "THz-frequency spectroscopic fingerprinting" of biological molecules for detection, identification, and classification applications. In Phase II a completely functioning nanofluidic sensor platform was developed, tested, and refined in combination with a significantly modified THz spectroscopic system. The focus of Phase II project was developments of inexpensive, microfluidic technology to fabricate disposable devices. The subsystem for circulating liquid through

15. SUBJECT TERMS
SBIR Report

16. SECURITY CLASSIFICATION OF:			17. LIMITATION OF ABSTRACT	15. NUMBER OF PAGES	19a. NAME OF RESPONSIBLE PERSON
a. REPORT	b. ABSTRACT	c. THIS PAGE			Tatiana Globus
UU	UU	UU	UU		19b. TELEPHONE NUMBER 434-296-2400

Report Title

Development of a Biosensor Nanofluidic Platform for Integration With Terahertz Spectroscopic System

ABSTRACT

Report delivered under topic #CBD 10-110, contract W911NF-12-C-0046.
The goal of this project is demonstration of a nanofluidic sensor platform effective for label-free "THz-frequency spectroscopic fingerprinting" of biological molecules for detection, identification, and classification applications. In Phase II a completely functioning nanofluidic sensor platform was developed, tested, and refined in combination with a significantly modified THz spectroscopic system. The focus of Phase II project was developments of inexpensive microfluidic technology to fabricate disposable devices. The subsystem for circulating liquid through the arrays of a micro/nano fluidic sample device was integrated into the spectrometer system. Significant system modifications included: a new data acquisition system and software; a new fluidic chip holder designed with a syringe pump driving mechanism; control system to allow flow through a microfluidic sample analysis chip; an automated height positioning of the probe. The accuracy and reproducibility of our system performance for background and sample characterization was evaluated. The theory has been developed to evaluate the dielectric permittivity of water and biomaterial solutions in the THz region for designing microfluidic channels and for data analysis. Protocol was developed for spectroscopic characterization of biomaterials using nanofluidics. Experimental characterization of sub-THz transmission spectra from DNA solution using microfluyidics demonstrated extremely high sensitivity of spectrometer with microfluidic chips in sub-THz range required less than 0.01 ng of dry material. The developed highly sensitive biosensors operating at room temperature with significantly improved ability to discriminate between species and to monitor interactions between biomaterials and reagents in near real-time opens the possibility of a single macromolecule and cell detection and identification and other applications, including material and agent sensing for identification and classification in defense and security, biomedical, pharmaceutical, food quality, and environmental control.

Enter List of papers submitted or published that acknowledge ARO support from the start of the project to the date of this printing. List the papers, including journal references, in the following categories:

(a) Papers published in peer-reviewed journals (N/A for none)

Received		Paper
06/26/2014	1.00	Masudur Rahman, Boris Gelmont, Michael L. Norton, Tatiana Globus, Igor Sizov. Sub-THz spectroscopic characterization of vibrational modes in artificially designed DNA monocrystal, Chemical Physics, (11 2013): 121. doi: 10.1016/j.chemphys.2013.08.015
TOTAL:	**1**	

Number of Papers published in peer-reviewed journals:

(b) Papers published in non-peer-reviewed journals (N/A for none)

Received		Paper
TOTAL:		

Number of Papers published in non peer-reviewed journals:

(c) Presentations

Number of Presentations: 0.00

Non Peer-Reviewed Conference Proceeding publications (other than abstracts):

Received	Paper

TOTAL:

Number of Non Peer-Reviewed Conference Proceeding publications (other than abstracts):

Peer-Reviewed Conference Proceeding publications (other than abstracts):

Received		Paper
06/26/2014	2.00	Jerome P. Ferrance, Alexander Khromov, Aaron Moyer, Tatiana Khromova, Boris Gelmont, Igor Sizov, Tatiana Globus, Mark A. Druy, Richard A. Crocombe. Portable sub-terahertz resonance spectrometer combined with microfluidic sample cell, SPIE Defense, Security, and Sensing. , Baltimore, Maryland, USA. : ,
06/26/2014	3.00	Tatiana Globus, Aaron Moyer, Boris Gelmont, Tatyana Khromova, Igor Sizov, Jerome Ferrance, Mehdi F. Anwar, Thomas W. Crowe, Tariq Manzur. Sub-terahertz resonance spectroscopy of biological macromolecules and cells, SPIE Defense, Security, and Sensing. , Baltimore, Maryland, USA. : ,
TOTAL:	**2**	

Number of Peer-Reviewed Conference Proceeding publications (other than abstracts):

(d) Manuscripts

Received	Paper
06/26/2014	4.00 Tatiana Globus, Igor Sizov, Boris Gelmont. FD 171: Sub-THz specific relaxation times of hydrogen bond oscillations in E.coli thioredoxin. Molecular dynamics and statistical analysis., Faraday Discussion (03 2014)
TOTAL:	**1**

Number of Manuscripts:

Books

Received	Book
TOTAL:	

Received	Book Chapter
06/26/2014	5.00 T. GLOBUS, B. GELMONT and I. SIZOV. Overview of terahertz spectral characterizationfor biological identifi cation, Woodhead Publishing: Elsivier, (07 2014)
TOTAL:	**1**

Patents Submitted

Patents Awarded

Awards

Graduate Students

NAME	PERCENT_SUPPORTED

FTE Equivalent:
Total Number:

Names of Post Doctorates

NAME	PERCENT_SUPPORTED

FTE Equivalent:
Total Number:

Names of Faculty Supported

NAME	PERCENT_SUPPORTED

FTE Equivalent:
Total Number:

Names of Under Graduate students supported

NAME	PERCENT_SUPPORTED

FTE Equivalent:
Total Number:

Student Metrics

This section only applies to graduating undergraduates supported by this agreement in this reporting period

The number of undergraduates funded by this agreement who graduated during this period: .....
The number of undergraduates funded by this agreement who graduated during this period with a degree in science, mathematics, engineering, or technology fields:.....
The number of undergraduates funded by your agreement who graduated during this period and will continue to pursue a graduate or Ph.D. degree in science, mathematics, engineering, or technology fields:.....
Number of graduating undergraduates who achieved a 3.5 GPA to 4.0 (4.0 max scale):.....
Number of graduating undergraduates funded by a DoD funded Center of Excellence grant for Education, Research and Engineering:.....
The number of undergraduates funded by your agreement who graduated during this period and intend to work for the Department of Defense .....
The number of undergraduates funded by your agreement who graduated during this period and will receive scholarships or fellowships for further studies in science, mathematics, engineering or technology fields: .....

Names of Personnel receiving masters degrees

NAME

Total Number:

Names of personnel receiving PHDs

NAME

Total Number:

Names of other research staff

NAME PERCENT_SUPPORTED

FTE Equivalent:
Total Number:

Sub Contractors (DD882)

Inventions (DD882)

Scientific Progress

A completely functioning nanofluidic sensor platform was developed, tested, and refined in combination with a THz spectroscopic system. The project was focused on further developments of an inexpensive nanofluidic technology toward future commercialization and fabrication. The efforts were aimed for stand-alone operation with sample injection and fluidic control built into the platform to facilitate transparent operation by the user. Micro/nanofluidic chips technology was developed, including a cover technology over the active area and integrating active region into total sample analysis chip. Instrumentation for automated flow control was developed and implemented. Interface packaging of fluidic platform with THz spectroscopic system was created. THz spectroscopic system was modified including: i) a new data acquisition system and software using National Instrument multifunctional module; ii) a new fluidic chip holder designed, fabricated and assembled with a syringe pump driving mechanism; iii) control system to allow flow through a microfluidic sample analysis chip; iv) a new detector housing to be combined with a micro/nanofluidic platform; v) an automated height positioning of the probe. The completed system was tested and evaluated. A new protocol was developed for spectroscopic characterization of biomaterials using nanofluidics. Spectroscopic characterization of biological materials in solutions was performed. Theory was developed to analyze experimental data and to calculate absorption coefficient spectrum from transmission measurements in nanofluidics. Experimental characterization of sub-THz transmission spectra from DNA solution using microfluyidics demonstrated extremely high sensitivity of spectrometer with microfluidic chips in sub-THz range that required less than 0.01 ng of dry material. from solution with concentration less than 0.1 %.

See Attachment.

Technology Transfer

Final Technical Report

Development of a Biosensor Nanofluidic Platform for Integration with Terahertz Spectroscopic System

The Department of Defense, Phase II Chemical Biological Defense Small Business Innovative Research (SBIR)

Proposal Number: C2-0358 (ARO Proposal No 62043ELSB2.)

PROJECT: CBD10-110

Contract W911NF-12-C-0046

Dates covered: March 28, 2012-March 27 2014

Authors: T. Globus (PI) [1], J. Ferrance[1], A. Moyer[1], M. Levi [1], I. Sizov[1], B. Gelmont[2], H. Powell[2], A. Lichtenberger[2].

[1]Vibratess, LLC, 104 Chaucer Road, Charlottesville, VA 22901
[2]Consultant, Department of Electrical and Computer Engineering, University of Virginia, VA 22904

Table of Content

Overall Project Goal:

The goal of this project is demonstration of a nanofluidic sensor platform effective for label-free "THz-frequency spectroscopic fingerprinting" of biological molecules for detection, identification, and classification applications. The efforts will aim for stand-alone operation with sample injection and fluidic control built into the platform to facilitate transparent operation by the user.

Our major objective in this research project is development of a nanofluidic sensor prototype packaged to be readily interfaced with THz spectroscopy systems, including systems that are commercially available. One of our key objectives is to achieve stand-alone operation with sample injection, fluidic and electrophoretic control that is self-sustained in a single enclosure to facilitate transparent operation by the user.

Specific objectives:

Objective I. Nanofluidic chips technology development including a cover technology over the active area and integrating active region into total sample analysis chip.

This objective will utilize the Phase I results, which define what is needed in the active area, and develop a method for fabricating this active area in a robust and inexpensive device. This work will integrate the detection region into a chip that will allow for both, sample and reference, solutions introduction and flow through the periodic structure. The also includes further development of inlet and outlet channel technology and the technology for covering the active area.

Objective II. Develop and implement instrumentation for automated flow control.

This aim will determine the necessary instrumentation components that will be used to control flow of samples and reagents through the devices. It will also define the sample chip interface device that allows it to interact with the instrumentation. This aim will use electrophoretic and electroosmotic flow to move material into and through the active area to allow for sample to be injected and washed out of the detection region. Initial work will utilize external syringe pumps, but integration of the pumping mechanism into the interface device is the ultimate goal of this effort.

Objective III. Development of interface packaging nanofluidic platform with THz spectroscopic system and required system modifications.

This aim will address the modification to the THz spectroscopy stage and, particularly, sample holder needed to accommodate the new microchip integrated into the interface device. The automated positioning of the detection probe capabilities in the vertical direction (Z-axis positioning) above the surface of the microchip will be developed to eliminate the need for extensive manual adjustments prior to measurements. This aim will also focus on modifications required in the software to control the automated movement of the sample, as well as redesign of the user interface to reduce the need for operator interaction during sample analysis.

Objective IV. System testing and evaluation**.**

This aim will focus on extensive testing and characterization of the instrument performance to demonstrate that the prototype system meets specified parameters, including reproducibility, sensitivity, special and spectral resolution, and the capability to resolve spectroscopic features from bio materials. Specification requirements for the nanofluidic platform combined with a spectroscopic instrument will be finalized during Optional Period of the Phase I.

Objective V. Spectroscopic characterization of biological materials using nanofluidic chips.

In the Phase I we were able to characterize biological materials only in the solid state after drying in channels. We could not match sample and background spectra since channels were not covered and it was not possible to control the amount of liquid during measurements. Phase I provided proof of principle that

we could construct and cover the necessary nanofluidic chip for characterization of biomaterials in solutions as part of this Objective. Construction of new nanofluidic chips with two inlets will also permit us to study and characterize biological and biomedical processes. We will perform measurements of signal which depend on frequencies (spectral characterization) and depend on time (kinetic of processes).

Objective VI. Development of stand-alone operation and general characterization of bio-materials in collaboration with DOD research center/laboratory**.**

Possible design of a system including stand-alone operation will be discussed during the Optional Period of Phase I in conjunction with a U.S. Army or DoD research center or laboratory that possesses expertise in bio-material/agents production, handling, and general characterization capabilities. The developed nanofluidic sensor will be packaged to be readily interfaced with a terahertz spectroscopic system which is commercially available.

Expected Impact of the Research**:** Successful implementation of the nanofluidic sensor platform will provide an opportunity for THz-frequency spectroscopic label-free fingerprinting of biological materials and agents. A new and deep understanding of the interaction between THz radiation and biomaterials will become possible and open the door to development of all optical, highly sensitive biosensors operating at room temperature with significantly improved ability to discriminate between species and to monitor interactions between biomaterials and reagents in near real-time.

Possible Applications:
In addition to the primary applications in biological material and agent sensing for identification and classification in defense and security, this technology development will impact the entire range of biological, biomedical, pharmaceutical, food quality, and environmental applications, with a new technology for studying protein and DNA conformational changes and small molecule drug interactions in ways never before possible.

Summary

The goal of this project is demonstration of a nanofluidic sensor platform effective for label-free "THz-frequency spectroscopic fingerprinting" of biological molecules for detection, identification, and classification applications. In Phase II a completely functioning nanofluidic sensor platform was developed, tested, and refined in combination with a significantly modified THz spectroscopic system. The focus of Phase II project was developments of inexpensive microfluidic technology to fabricate disposable devices. The subsystem for circulating liquid through the arrays of a micro/nano fluidic sample device was integrated into the spectrometer system. Significant system modifications included: a new data acquisition system and software; a new fluidic chip holder designed with a syringe pump driving mechanism; control system to allow flow through a microfluidic sample analysis chip; an automated height positioning of the probe. The accuracy and reproducibility of our system performance for background and sample characterization was evaluated. The theory has been developed to evaluate the dielectric permittivity of water and biomaterial solutions in the THz region for designing microfluidic channels and for data analysis. Protocol was developed for spectroscopic characterization of biomaterials using nanofluidics. Experimental characterization of sub-THz transmission spectra from DNA solution using microfluyidics demonstrated extremely high sensitivity of spectrometer with microfluidic chips in sub-THz range required less than 0.01 ng of dry material. The developed highly sensitive biosensors operating at room temperature with significantly improved ability to discriminate between species and to monitor interactions between biomaterials and reagents in near real-time opens the possibility of a single macromolecule and cell detection and identification and other applications, including material and agent sensing for identification and classification in defense and security, biomedical, pharmaceutical, food quality, and environmental control.

Introduction

The goal of this Project is to develop a completely functioning micro/nanofluidic sensor platform in combination with a THz spectroscopic system. The major focus of this Phase II work was developments on the inexpensive micro/nanofluidic technology toward future commercialization and fabrication of an associated interface device to provide a packaged platform.

Two different technologies were used in the Phase I effort for concept demonstration. In one of them we used a multichannel array devices developed and fabricated by our subcontractor at UVA, Dr. A. Lichtenberger. These high quality devices based on semiconductor technology to produce thin film SiN in a frame of monocrystalline Si satisfied all requirements. The technology, however, is complicated and expensive. We also tested devices fabricated by our subcontractors in previous projects, Redondo Optics, PI-E. Mendoza, and UVA subcontractor, PI- Dr N. Swami. The quality of these devices made on plastic polymethyl methacrylate (PMMA) substrates was not satisfactory for one or other reason. By the start of the Phase II, it became clear that with the goal of developments inexpensive micro/nanofluidic technology toward future commercialization and fabrication of an associated interface device to provide a packaged platform, we have to bring the technology in-house, so we have more control over the design, materials, and cost of the devices we were developing. Thus the decision was made to organize the Vibratess technological laboratory equipped with the all necessary facilities. This activity became our first goal, heavily consuming time and resources of the Phase II project, before we could start the device technology development. It included not only the choice and ordering of equipment but also testing, modifications and adjusting.

Additional task

In preparing for developing the fabrication technology, we identified and ordered the instrumentations needed to construct the micro/nanofluidic systems. The equipment for fabrication of the active area of the chips with the gold array and it sealing with a cover layer was purchased and additional laboratory space was selected for setting up the equipment. The laboratory facility leased for fabrication of the devices was outfitted with the necessary laboratory benches and desk space. The instrumentation for fabrication of micro/nano-fluidic chips including a Laser-Cutting System, a Sputtering system, a Spin Coating Processor, and a UV Exposure System was installed at the facility. Figure 1-1 shows the new facilities in the initial stage. The necessary auxiliary equipment, including an air compressor and computer were obtained, or constructed, including a surround for the UV exposure system to contain the UV radiation (Figure 1-2) and an exhaust surround for containing the spin-coater.

Figure 1-1. Dr. J. Ferrance working on a bench with technological equipment in the new laboratory facilities

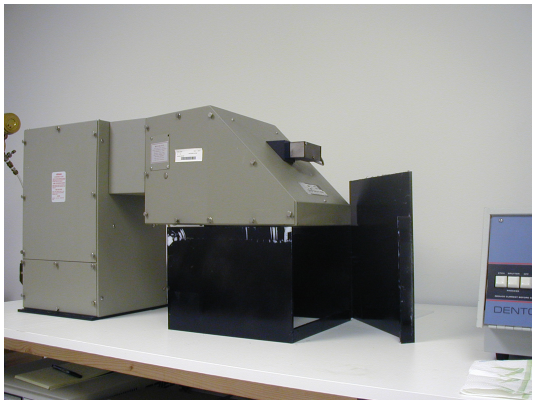

Figure 1- 2. Completed UV expose system with a surround to contain the UV radiation

Complete functionality of the instrumentation was confirmed and the initial fabrication steps demonstrated. Maintenance and repair of the instrumentation was required over the course of this project, including repair of the shutter in the UV exposure system, cleaning of the UV exposure system optics, and parts replacement in the sputtering system.

Initial testing with the laser cutter showed that the exact cutting and raster conditions (laser power, cutting speed) would have to be determined for most of the materials used in this project to generate the desired dimensions and accuracy with clean edges at the cuts. AutoCAD drawings were modified to account for holes ending up larger than necessary due to the width of the laser cut.

After initial fabrication development, it became clear that reproducible and accurate pattern transfer of the mask image to the photoresist was being compromised by the presence of dust in the laboratory. Construction of a clean area (shown in Figure 1-3) inside the technological laboratory was therefore performed to allow for better fabrication of devices with a reduced numbers of defects. A metal frame was designed and assembled. It was then covered with static resistant plastic (PVC) to serve as an enclosed work area. High efficiency particulate air (HEPA) filters and a blower were installed on an overhead plenum to supply very clean air to the enclosed area. All lithography work was subsequently performed inside the clean area. During the course of this work, a number of additional tools and components specific for use in this project were developed and implemented to provide a means to accomplish tasks required in the fabrication, use, and testing of devices.

Figure 1-3. Construction of a clean area facilities (includes two benches) in Vibratess' technological laboratory.

I. Micro-Nanofluidic chips technology development (Objective I)

The major focus of this project was development of micro-nanofluidic chips technology. This work included three major different sub-tasks. The first is developing reliable technology for a fluidic array of channels in a metal layer on a plastic substrate. The second is developing a cover technology over the active area. The third is integrating the active region into a complete sample analysis chip.

Subtask 1.1 Design and fabrication of inexpensive, robust micro/nano-fluidic chips on plastic substrate

Microarrays with dry film photoresist technology

The first subtask is the development of technology for manufacturing inexpensive (disposable) microfluidic chips on plastic substrate to be used with sub-THz spectroscopic system of nano-gram samples for bio-material characterization. These devices having periodic pattern of microchannels in a metal layer will fulfill two functions: hold biomaterial sample for characterization and enhance interaction of radiation with a sample material to enhance the sensitivity. This is a rather complicated task because although plastic is transparent in this range, it is a soft material, not allowing the use of high temperature and, in addition, has a very poor adhesion with metal. Initial development of technology has been

performed by our subcontractors in previous projects and in a Phase I of this project. The results of two subcontractors were not satisfactory: too many defects were present in the prototype samples, i.e. gold layer was not thick enough, adhesion with metal was not strong and it came off from a plastic substrate.

In initial stage of technology development we replaced the previously used thicker (175 um) PMMA substrate with thinner (50 um) polyester (PET) substrate, as PET is more chemically and thermally resistant, and can be readily obtained in a variety of thicknesses down to 12.5 um, sputtered a gold seed layer on the PET, and replaced the SU-8 resist with Dry Film resist (DuPont Riston FX920). This technology excluded organic chemicals, reduced the processing temperature and eliminated overheating and shrinking of a plastic substrate. The basic method of array production remained the same, with a gold seed layer being applied to the substrate, then a photoresist applied. The photoresist was patterned using a photomask by exposure to UV irradiation, then developed to leave the patterned resist on the surface. Gold was then electroplated onto the substrate around the photoresist pattern to the desired thickness. Removal of the photoresist and removal of the seed layer results in open channels in the deposited gold which form the microchannel array structure. To provide for eventual connection of the array into a larger microfluidic device, open areas were designed into the mask at the ends of the microchannel array to allow for distribution of the liquid into all of the microchannels with a larger inlet and outlet channel extending from the open areas.

In this initial work, it proved difficult to produce a gold seed layer which sufficiently bonded to the PET to perform a subsequent gold electrodeposition step, even with a chrome adhesion layer between the PET and gold layer. In addition, neither of the two dry film photoresists from DuPont selected for use in this project bonded well with the gold layer. Further work on evaluating the two dry film photoresists resulted in selection of one resist as better suited for this project, and showed that it was possible to produce useful arrays using a lift off method. In the lift-off method, the dry film photoresist was applied directly to the PET substrate, then patterned and developed, which was followed by sputtering of gold over the entire substrate. When the photoresist was stripped away, the gold over the resist was lifted off, while the gold deposited directly on the substrate remained. This produced a gold array of microchannels on the surface of the PET.

The quality of the produced lift off devices was already much better in comparison with those produced by previous sub-contractors (UVA and Redondo Optics). The drawbacks were the long time required for the sputtering or evaporation processes since it may take several hours, and the amount of gold wasted in the process. Thus, while the lift off process was proven successful, this method for array fabrication was not optimal and technology development continued.

The dry film resist was designed for use on a copper surface, and the use of copper would make the final devices much less costly to produce and sell. Simulation also indicated that copper should function as well as the gold, if not better, for radiation enhancement. Copper was therefore tested, and initial copper arrays were generated using the lift-off process, Figure 1-4 presents a photo of such a device.

It was more valuable, however, to utilize electrodeposition of copper to generate the arrays since the thickness of the copper is easily controlled by the time and current utilized in the deposition step. In addition, the electrodeposition process is much faster, and there is significantly less wasted metal compare to sputtering.

With the use of gold, there were two addtitional problems: poor adhesion of the gold seed layer to the PET, and the photoresist not sticking to the gold seed layer. For copper electrodeposition a number of different metals were investigated as potential seed layers for the copper deposition. In the end, a silver seed layer sputtered onto a PET substrate was stable, and made it possible to use the dry film photoresist to create the array pattern on the silver coated PET substrate. Copper was then electrodeposited to a thickness of 5 um around the photoresist. Once the photoresist was removed, the silver seed layer in the channels could be etched away, leaving the copper array. Because silver can be etched with a solution which does not etch copper, removal of the underlying seed layer does not affect the copper array. An image of an electrodeposited array is shown in Figure 1-5. Some defects in the array pattern are evident, due to adhesion between the silver and photoresist. This technology also produced useful arrays, but

consistency was not satisfactory and sometimes the electrodeposited copper layer would peel off of the silver seed layer.

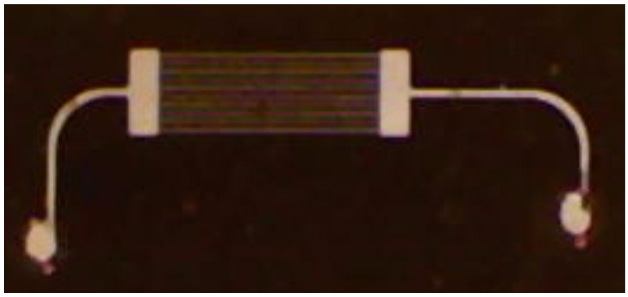

Figure 1-4. An inner layer of a microfluidic chip with inlet and outlet channels. Sputtering of a thick copper layer on a treated plastic without a seed layer using a dry photoresist and a direct photomask.

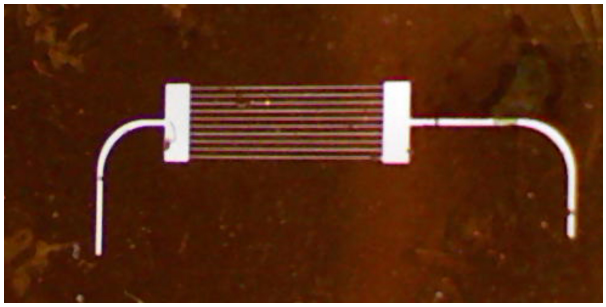

Figure 1-5. An inner layer of a microfluidic chip with inlet and outlet channels: electrodeposition of a thick copper (3-5 micron) on a silver seed layer using a dry photoresist and a direct photomask has been made.

Fabricating the copper arrays through etching of a prefabricated copper film using microspray photoresist.

In addition to the lift-off and electrodeposition processes for forming arrays, technology was also tested to evaluate an etching method for forming arrays. For this method, the photoresist must be exposed using a reverse photo mask, exposing the areas in the metal to be removed to form the channels. In this method, a prefabricated metallic foil of necessary thickness adhered to a plastic substrate would be etched to form the microchannels in the array. Initially, a 12 um thick copper foil tape was obtained from Bare Metal Foil Co., which could be adhered to a PET substrate then covered with the dry film photoresist. Following UV exposure through a reverse mask, the patterned photoresist was removed where the channels and open areas were desired, allowing the underlying copper to be etched away. Two issues arose at this point, the first was that the dry film photoresist did not have a high enough resolution to pattern the fine features required to etch the arrays. The second issue was that the copper tape was not pure copper, but an alloy, and thus did not etch cleanly.

The first issue was addressed by replacing the dry film resist with a spray on photoresist available from Microchem Corp (called Microspray). The Microspray positive photoresist requires a relatively low processing temperature, allows the thickness of the photoresist to be controlled by the number of layers applied, and can provide a resolution better than 1 um. Since this photoresist (and most liquid resists) was designed for use with silicon, not polymer substrates, processing conditions had to be adapted for use in this method. Because of the better resolution of the resist, a new mask was also needed with feature sizes adapted for the new resist. In addition, one of the issues we indicated as needing addressed in our original proposal was the need to incorporate markings into our design which would allow for identification of the exact position of the probe within the array. In the design of this and subsequent masks, crosses were incorporated into the spacers between channels in specific locations which allow for identification of the position of the probe within the array.

The second issue, of the copper tape not being pure copper, was addressed by the identification of a DuPont material called Pyralux, which is a 25 um thick polyimide substrate covered on both sides with a 5 um thick copper layer. This thickness is closer to what was desired in the height of these arrays. We developed a method to fabricate the copper arrays by etching a copper film laminated on a polyimide substrate using a spray-on positive photoresist to generate an etch mask. Pyralux pieces were sprayed with the new photoresist then patterned using UV exposure through the new mask. The copper on the back side of the polyimide was completely removed by etching, then the array was formed by applying

copper etchant over the patterned photoresist. As soon as light was visible through the microchannels, the etching process was stopped.

This technology has several advantages, the most important being a reliable bonding of a metal to a polyimide substrate. It is also inexpensive. Besides, THz transmission is high and hydrophilic surface is very good. This technology proved to be a fast and convenient method for fabrication of arrays, with the use of a commercially available substrate eliminating a significant number of fabrications steps from the process. Test measurements have shown that the fabricated devices can be used for biomaterials characterization. However, several serious problems have been identified, including the striated structure in the copper film and difficulties to control the channels width due to a deep etching of the copper film. Indentations in the original copper layer laminated onto the polyimide (from High Performance Copper Foils) with the width about 2-3 um, as well as the grain structure of the copper shown in Figures 4-1(a) and 4-1(b) of subtask 4-1, make it difficult to reproducibly fabricate the specified narrow width of channels, and the technology can not be used for nanofluidics. To control the channel width in these etched devices, the channel images in the newest mask have been reduced to 4 um wide. Nevertheless, these negative factors required further technology improvement. For all these reasons we continued development of a different approach using the electrodeposition of copper to form arrays on polyimide sheets.

Alternative polymer substrate materials and using liquid photoresist

The determination that polyimide could be used as a good polymer substrate rather than PET, provided additional benefits for the fabrication of arrays. Literature reports identified methods to treat polyimide for fabrications of copper structures up to 30 um thick, suggesting that plasma treatment of the polyimide, followed by evaporation of a chrome and copper seed layer would allow for good electrodeposition of copper without delamination of the deposited copper from the substrate. A commercial thin film deposition provider was identified (Newport Thin Films, Inc.), who could take supplied polyimide and perform the plasma treatment, chrome, and copper depositions, all under vacuum to prevent surface contamination. Initial attempts to electro-deposit copper onto this material, however, showed that the vapors from the deposition solution attacked the copper seed layer where it made contact with the electrode. To eliminate this problem, a silver layer was sputtered over the copper seed layer, only where the electrode contact was made. Once this modification was incorporated, devices were routinely fabricated by patterning of the spray-on photoresist over the copper seed layer followed by electrodeposition of copper to the desired thickness. The photoresist could then be removed from the channels and open areas and the copper seed layer etched away, followed by etching of the chrome adhesion layer. Chrome layer etching proved to be a challenge, as most chrome etchants will preferentially etch copper. A specific etch formula was therefore researched and prepared for removal of the chrome layer without attacking the copper.

Using either etching of Pyralux or electrodeposition of copper over a copper/chrome seed layer on polyimide, made it possible to create inexpensive disposable arrays for THz radiation concentration on polymer substrates. Explorations to determine improvements to this technology did continue however. Our original array design utilized 10 channels, but the sensitivity through this array was determined to be not sufficient. A new mask was designed and is now in use which contains 21 channels; copper posts were also added in the open areas in this mask design for better cover attachment as described in Task 1.2.

Evaluation of the technology, which utilized the spray-on resist, has revealed several significant quality issues with the channels in the microchip's periodic structure array. It was imperative to eliminate the grain structure of the copper in the array and improve the reproducibility of the channel widths and sharpness of channel edges. During the electrodeposited copper etching step, surface imperfections were detected, and a new compound microscope was purchase from AmScope, having 40X to 1000X magnification capabilities to better visualize array features and irregularities, which were isolated to the photoresist process. Figures 1-**6a** and 1-**6b** demonstrate imaging capability of the compound microscope for sprayed photoresist (before development) with 35sec and 60sec exposures. A trinocular head allows

attachment of a camera to the microscope for image capture that allow a comparative analysis to be made later. Correcting all of these deficiencies should improve the effect of radiation concentration in the channels, the measurement sensitivity and the results reproducibility. Work continued for controlling the thickness, processing of the photoresist and controlling the exposure conditions that are important in obtaining structures satisfying the requirements for the necessary widths and sidewalls of channels.

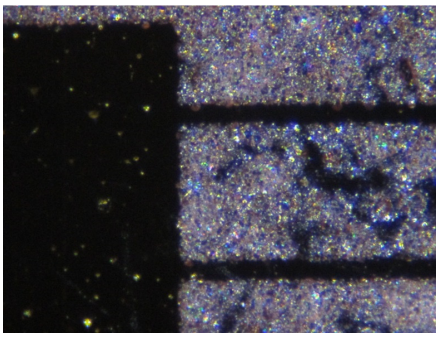

Figure 1-6a. 35 sec exposure (photoresist before development)

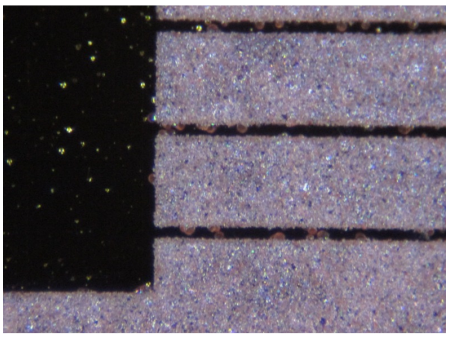

Figure 1-6b. 60 sec exposure

A major improvement was the replacement of the spray-on photoresist with a liquid positive photoresist from Microchem (SPR220-7.0), which could be spun on to give a more consistent and reproducible 10 um thick layer of photoresist. The utilization of a spin-coating procedure for photoresist application, rather than the spray-on photoresist, not only provides better reproducibility but also allow us to further reduce the channel widths and move from microfluidic toward nanofluidic microchips.

We had developed processes for using the spin on photoresist with the metal coated polyimide substrates to give a more consistent and reproducible 10 um thick layer of photoresist. To use our thin flexible substrate in a spin-coater, we have to mount the substrate to a rigid structure to hold the polyimide substrate flat during the spin coating procedure. The method was mediated by a literature report of using polydimethylsiloxane (PDMS) coated glass slides to hold thin polymeric sheets flat, thus allowing them to be used in a spin coater. We determined the required conditions to coat glass slides with PDMS using the spin-coater and then cured the PDMS to provide a thin, flat layer about 50 um thick. Polyimide substrates flatten out and adhere to the PDMS layer due to van der Waal forces. To help position the glass slides on the spin-coater consistently, which is required for balanced operation of the spin-coater, a centering jig was constructed specifically for this purpose.

The introduction of the spin on resist for patterning the array channels required some optimization of the processing conditions for the photoresist. This included the soft bake time, exposure time, hold time, post exposure bake time and temperature, and the choice of developer. Figures 1-7 and 1-8 show patterned photoresist using a post-exposure bake with no wait time and with a 60 min wait time after exposure. Using the best conditions that we developed for producing sharp features in the spin on photoresist, we fabricated arrays by electrodepositing copper onto the copper seed layer and after then removing the photoresist to expose the channels in the copper. Work with this photoresist included evaluation of both the patterned photoresist and the subsequently deposited copper features. Optical evaluation of the arrays being produced by the photoresist patterning and subsequent copper electrodeposition methods allowed us to ensure vertical channel walls for THz radiation enhancement as shown in Figure 1-9.

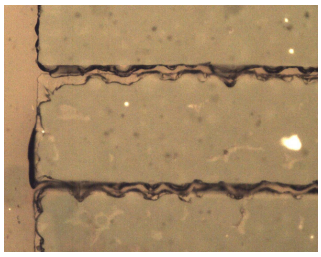

Figure 1-7. Patterned photoresist after development. Photoresist was baked at 115˚C right after exposure.

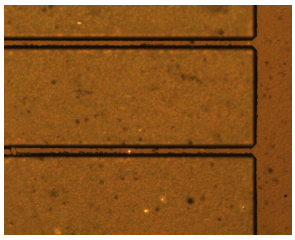

Figure 1-8. Post exposure bake was delayed for 60 minutes

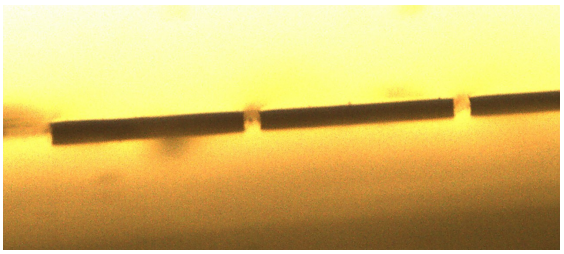

Figure 1-9. Microscope images looking into the ends of the channels in the array show vertical sidewalls and sharp transitions.

Based on the development of final processing conditions, a Standard Operating Procedure (SOP) manual was prepared to define the fabrication technology. Figures 1-10a and 1-10b (as example from the SOP manual) show the process of placing a glass slide on the spin-coater using the centering jig.

Figure 1-10a – Spin-coater with its hood raised

Figure 1-10b – Placing glass slide over spin-coater shaft using the centering jig

As part of the continuing development efforts, additional seed layers were also investigated, having polyimide coated with both chrome/silver and chrome/gold to see if these seed layers would improve processing of the arrays. Neither has been as successful as the copper/chrome seed layer material. The use of other polymeric substrates has also been investigated, having our commercial coating supplier also plasma treat and chrome/copper coat polycarbonate, polyester, and polymethylmethacrylate. Issues of delamination remain with the PET substrate, and the polymethylmethacrylate is not compatible with the processing conditions used for fabricating the arrays. The polycarbonate, however, has been successfully used to make arrays, but surface roughness is an issue now being explored, as this substrate could potentially work better than the polyimide currently being used.

As indicated above, cross marks were incorporated into the array design to allow for identification of specific locations within the array. At the same time, the issue of repeatability of positioning of arrays into the spectrometer was also addressed by the development of frames onto which the arrays are mounted for placement into the spectrometer. By more precisely positioning the array onto the frame structure, it is now possible to repeatable position the arrays within the spectrometer, such that the same channel is always presented to the probe in each array. To achieve this, a precision film cutter was designed and constructed which helps in lining up the arrays within the frame, and a vacuum system was constructed to hold the array exactly in place while the frame is attached. Both of these devices are also utilized in the construction of the complete microfluidic devices detailed under task 1.3.

Nanoarrays techmology development

All of the arrays work described above focused on the fabrication of 10 um wide channels spaced on 150 um centers. One of the requirements in the original call for proposals, however, was the investigation of nanofluidic channels, where the width of the channels is less than 1 um wide. To achieve these arrays, we collaborated with our consultant on the Phase I effort, Dr. Lichtenberger.

The obstacles confronting realization of such a submicron channel in 3-5 um thick metal fields are significant. Reactive ion etching, which is often used to realize sub micron sized features, is not appropriate in such thick films. Plating of metal films into resist features presented itself as a likely alternative. Forming channels by plating implies the definition of the nominal channel width (and height) in the resist feature. So a 0.5 micron wide resist feature should realize a 0.5 micron wide channel. However, two realities are immediately confronted. The first is the difficulty in defining a submicron wide line in resist >2 um thick with traditional contact aligners. The second is the reality that in the process of plating, the plated metal typically impinges on the defining resist feature and plates under that feature to some extent. A 0.5 micron wide resist feature may end up being "squeezed" by the plating process and be removed entirely- resulting in the entire field being plated with no channel present.

To achieve sub micron channels, Dr. Lichtenberger developed multistep electroless plating approach initially using a quartz substrate. The substrate was ion etched, then coated with a titanium adhesion layer and a gold seed layer. The photoresist was applied and patterned using the same design as for the 10 um wide channels, but with channels defined at a width of 1.8 um. An array of 1.8 um wide channels was then produced by electrodepostion of nickel around the photoresist as was done with copper in the wider channel arrays. Once the nickel was deposited, the resist was removed and the seed layer and adhesion layers were removed. To narrow the channel width, additional nickel was then deposited using an electroless deposition method, in which nickel will deposit on the nickel already present, but not on the substrate. The time for deposition was controlled to deposit an addition 0.2 um of nickel to the surface. This was followed by an electroless deposition of gold to a thickness of 0.3 um. This increase in the deposited metal thickness of 0.5 um on both sides of the channel resulted in a channel, which was 800 nm wide in the final array. This double electroless plating scheme was investigated with a test mask and ultimately proved to be succesful. Figure 1-11 shows an SEM image of a submicron channel width, 2um in thickness using this new process.

In the next step, Dr. Lichtenberger investigated the application of this new electroless channel formation process to thin polyimide substrates. The flexible substrates impact the process in a number of ways, including issues of ion etching, photoresist baking, exposure and removal, and electrodeposition which were solved. A new mask set, with full channels, mixing section and source/drain feeds has been designed and manufactured. The first prototype samples were realize at the end of this reporting period. Figures 1-12 and 1-13 show the nanochannels fabricated on polyimide substrate by Dr. Lichtenberger. This method can now be used to successfully fabricate nanochannel arrays for incorporation into microfluidic devices. Although not as inexpensive as the microchannel arrays, the technology is straightforward and uses methods commonly employed in the microfabrication industry.

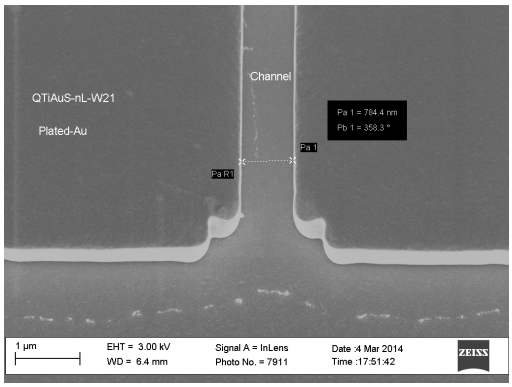

Figure.1-11. SEM image of a submicron channel width, 2um in thickness using this new process.

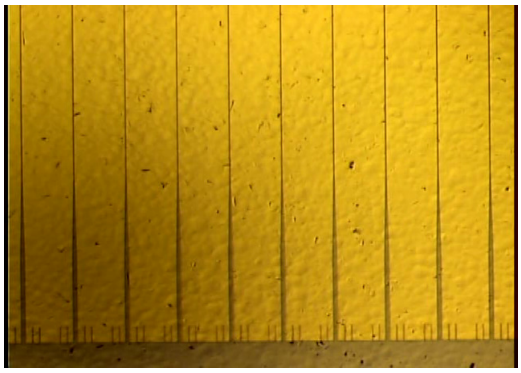

Figure. 1-12. Tapered channels leading to the submicron channel widths. At the bottom, there are four 'dummy' test channel features of different width for calibration purposes.

Figure 1-13. View of one of the channels in a solid Au field.

Conclusions for Task 1.1.

Task 1.1 represented a significant portion of the research performed under this Phase II effort, toward the development of technology to produce inexpensive arrays on polymeric substrates for THz radiation concentration that are ready for commercial development. We evaluated a number of materials and processing method, and have developed three potential technologies – a lift off process, an etching process, and an electrodeposition process - that can be commercially employed to produce disposable microchannel arrays for incorporation into microfluidic devices. In addition, through the help of our consultant, we have successfully developed a method for the production of nanochannel arrays that should also be scalable for commercial development.

Subtask 1.2 Developing a cover technology over active microfluidic area.

Cover attachment using a lamination adhesive

In the Phase I effort, we utilized a 6 um thick polycarbonate film as a cover layer over gold arrays, using epoxy to both bind the cover layer to the substrate and to define a surround around the array with inlet and outlet channels to allow fluid to enter the array. In that design, the cover was attached to the epoxy around the array, but not directly to the array itself, allowing for liquid to potentially pass over the top of the array. In the phase II effort, the surround and the inlet and outlet channels for liquid flow through the array were defined into the metal structure, which contained the microchannels. This meant that the cover would be directly attached to the surface of the metal, both around and over the microchannel array active area.

One of the goals was to make a cover layer less than 15 um thick to obtain near field effects, and two materials were available for that purpose: Polyester (PET) film 13 um and Polycarbonate (PC) film 6 □m thick. Films this thin with adhesive already on are not commercially available, thus an adhesive had to be found which could bond polymer to metal, and could be spread extremely thin since the array channels are only 5 um deep and the adhesive cannot fill the channels during the cover attachment step. In addition, a thick adhesive layer would also required the detection probe in the spectrometer to be further above the surface of the array, decreasing sensitivity and potentially causing issues with near field sensing.

Based on our requirements, Dow Chemical suggested the use of their ADCOTE 545-80 lamination adhesive. The choice of a lamination adhesive was based on the fact that the use of a liquid adhesive could flow into and fill the microchannels when the adhesive coated cover layer was applied. With the lamination adhesive, the adhesive is applied to the cover layer and allowed to dry, then heat activated to bond the surfaces together. Dow supplied us with a sample of this two component system, consisting of the ADCOTE 545-80 and Coreactant 9L10, which were to be mixed in specified proportions, and diluted

with 2-butanone solvent to the desired solids content. This adhesive was then spread to ~7 µm thickness on 13 um PET and 6 µm PC and allowed to dry. The cover material was then laminated over the arrays. Changes in the dilution, the thickness spread, and spread method, and the lamination temperature and pressure were all investigated to produce arrays in which the microchannels were not filled with adhesive, and liquid could flow through the array. After a number of attempts, success was achieved, but the adhesion was not homogeneous, and numerous air pockets could be observed across the surface of the bonded arrays. In addition, the long term stability was not good, with the polyester covers coming of when liquid flowed into the devices a few weeks after they were bonded. A number of other cover materials were tested, with polyimide and polyacrylic not working at all. The polycarbonate material worked well, but the 6 m thick PC was very difficult to work with. It was therefore decided to continue efforts to cover the arrays using the 13 um thick polyester film.

Cover bonding using other adhesives

On the devices formed by etching of Pyralux, the spray-on photoresist itself could be used as the adhesive and laminated directly to PET cover. Since the photoresist was already present, and patterned to have open channels, it was less likely to fill and clog the channels when the cover was applied. Various thicknesses of the photoresist, achieved by the number of sprays used, and different lamination temperatures were tested. Flow was observed through a number of devices bonded in this manner, but long term stability was an issue, and the photoresist was affected by a number of common fluids such as basic solutions and 2-propanol.

A number of additional adhesives, including epoxies, cyanoacrylates, UV activated acrylic adhesives, and spray on adhesives were tested for bonding of the covers to the copper arrays, but now worked as well as the ADCOTE adhesive.

New lamination adheisve formulation

Dow Chemical was contacted to determine if they could address the issues with bubbles and ageing of the adhesive. Dow responded with samples of two additional ADCOTE adhesives, and another Coreactant, Coreactant F. Since Coreactant F was also indicated with the original ADCOTE 545-80 adhesive, this combination was tested along with combinations of the new adhesives supplied by DOW. The original ADCOTE 454-80 adhesive with Coreactant F was found to have a much better bonding characteristic than the original formulation with Coreactant 9L10, and worked best of the combinations tested. Figure 1-14 compares the bonds between the two formulations, with the use of the new coreactant showing significantly less bubbles. This formulation also showed much better long term stability.

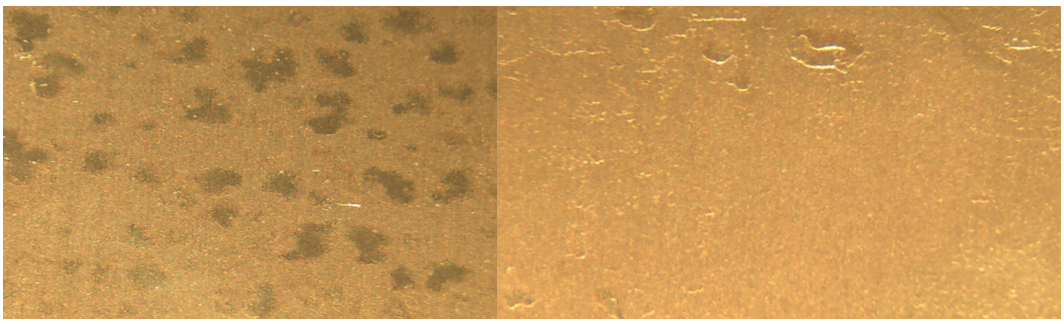

Figure 1-14. Left side shows bubbles between cover and copper layer using old ADCOTE formulation which are not seen in right image using the new ADCOTE formulation.

The bonding strength of this new formulation was also greatly improved. Previously, to fill the array with liquid, a vacuum was applied at the outlet of the array. With this new adhesive, pressure could be used to force liquid into the array microchannels without causing the cover to come free from the array.

Additional cover technology work

Implementation of the new liquid photoresist for fabricating arrays introduced application using the spin-coater with substrates supported on PDMS coated glass slides. This technology was also utilized for application of the lamination adhesive to the cover layer. Here, the PET cover was placed on the PDMS coated slides and the lamination adhesive spun to a consistent thickness. Optimization of the dilution of the ADCOTE adhesive was required, as the solvent evaporated much faster in the spin coater than when spread on the cover using a roller. In addition, the spin speed and timing had to be optimized for the spin coating process.

The open areas at the ends of the microchannel array are designed to allow for distribution of the liquid into all of the channels, but as seen in Figure 1-15, the area is large enough that the cover layer can actually be squeezed down and bond to the polyimide substrate during the lamination process. To address this issue, in the new 21 channel mask design, circular structures were incorporated into the open area, which form copper posts during the copper electrodeposition. A covered array with the new design is shown in Figure 1-16. The copper posts in the open areas help support the cover layer, prevent it collapse during bonding and help direct liquid flow through all of the channels.

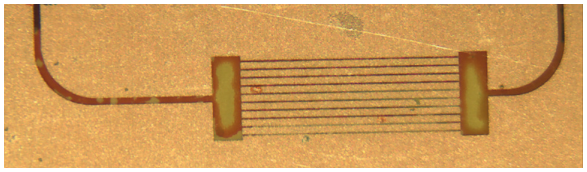

Figure 1-15. Liquid filled array (original design) showing collapse of the open areas during the bonding process.

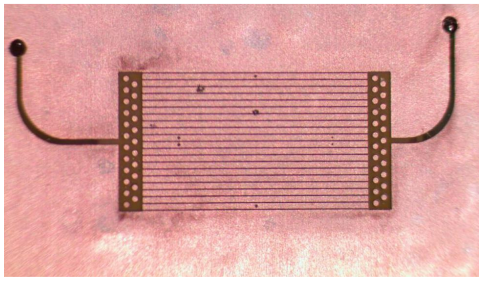

Figure 1-16. An array design with 21 channels, and posts in the open area to prevent collapse of the cover during the bonding process.

To allow for flow of liquid into the array in the completed devices, holes have to be fabricated through the polyimide layer before the cover layer is attached. Originally these holes were fabricated by hand using a small drill bit. Another of the tools developed was a punch designed specifically for preparing these inlet and outlet holes through the polyimide material. The holes produced by the fabricated punch are much cleaner and more easily positioned than those fabricated by hand with the drill bit.

Conclusions for Task 1.2

Task 1.2 also represented a major portion of the research effort in this Phase II project. It included not only finding an adhesive, that would bond strongly to both the metal array and the polyester cover, but could be spread thin enough to bond without filling the channels, and would be homogeneous enough to keep sample material in individual channels as it was passed through the array. **??** In the end, a technology was developed that could be reliable employed, and remained cost effective for the fabrication of disposable microfluidic devices.

Subtask 1.3. Integrate active region into total sample analysis chip

The microfluidic sample analysis device (a fluidic chip) is comprised of multiple layers of thin films that are bonded together. The complete device consists of a covered active area array along with the inlet and outlet channels, which allow the device to be integrated into a holder designed to fit into the spectroscopic instrument. Figure 1-17 shows the series of layers from which the completed device is constructed. The bottom layer, channel layer and intermediate layer are put together first and tested for fluid flow through the lower level channels. These layers are held together using an acrylic adhesive which comes precoated on the PET films being used to fabricate these pieces. As discussed in sub-Task 1.2, holes are punched through the polyimide support at the end of the array inlet and outlet channels before the cover layer is bonded over the array, to allow access to the channels in the copper array from the channels

in the bottom layers. The covered array is placed onto the vacuum alignment system which allows the holes in the polyimide layer to be aligned with the holes at the end of the lower channels in the intermediate layer. Initially, the top layer shown in Figure 1-17 was used to help hold the covered array in place.

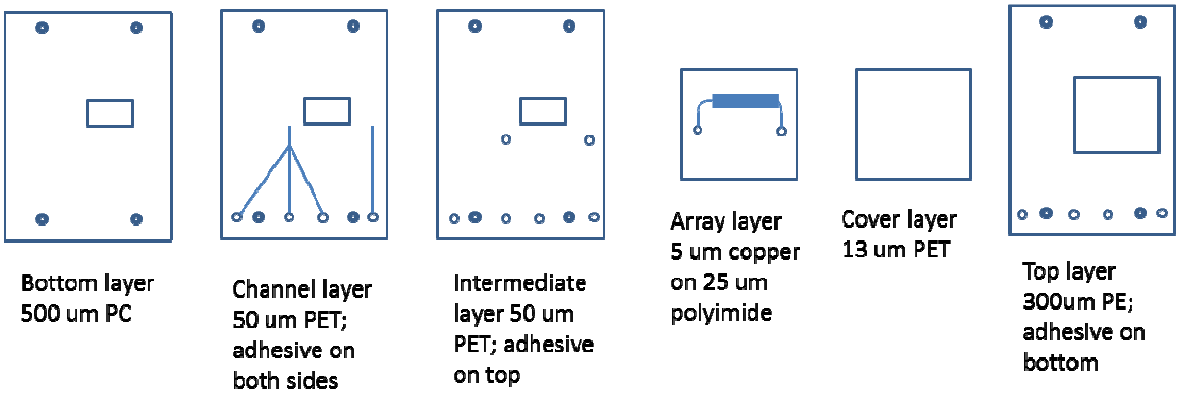

Figure 1-17. Drawings of the individual layers of the microfluidic device.

A photo of the completed device components is shown in Figure 1-18, including an assembled bottom section that contains the inlet and outlet channels (three first layers in Figure 1-17), on the left, a covered array layer shown in the middle on the Figure 1-18, and the top section (on the right) used to help hold the covered array in place. A picture of a completed microfluidic sample analysis device is shown in Figure 1-19.

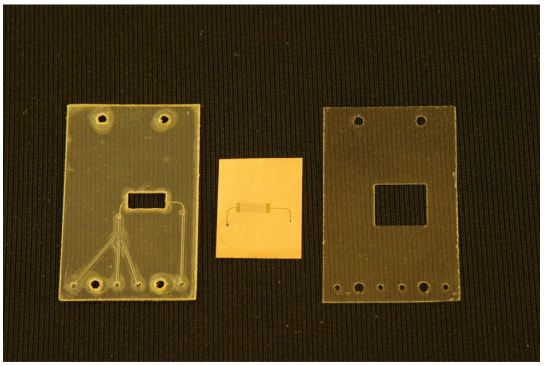

Figure 1-18. The complete device components: the bottom assembly component (on the left), the covered mucrofuidic array (in the middle), and the top layer (on the right).

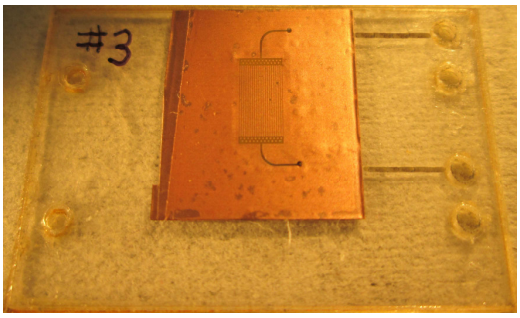

Figure 1-19. The completed microfluidic sample analysis device. Thick back frame (0.5 mm) supports device holding it flat.

Throughout the Phase II effort, some changes were made to the assembled device fabrication, but the design remained essentially the same as in the Phase I Research focused on optimizing the fabrication of these parts using the VersaLaser laser engraving system purchased for this project. Modifications in the speed and power requirements used for cutting each material were needed to regulate the sizes of the produced features and the amount of melting of the substrate observed around the cuts. Sizes of the open areas in the bottom layers were adjusted when the array size was increased from 10 to 21 channels, and tapering of the edges was included to provide more area for bonding. Originally, the covered array was bonded to the bottom layers using the acrylic adhesive precoated on the PET used to fabricate the intermediate layer. Once pressure driven flow was achieved through these devices, it was observed that this bond became the weakest point in the design with liquid leaking out between these two layer. Because of this, the pressure sensitive adhesive was replaced with the ADCOTE 545-80 lamination adhesive, which provided better bonding between the polyimide and the polyester intermediate layer.

Conclusions for Task 1.3

Research under Task 1.3 focused on optimizing fabrication conditions for these devices. The design and materials selection relied on previous microfluidic device fabrication experience within Vibratess, which allowed for easy implementation of the covered arrays into compete devices. The technology developed was cost effective for fabrication of individual devices, and the design can be readily incorporated into a larger scale mass production effort for production of disposable liquid sample analysis devices.

II. Develop and implement instrumentation for automated flow control (Objective II).

This objective includes the platform development for circulation of liquid sample solution into the sample arrays and Modification of THz Spectroscopic system to accommodate fluidic platform

Subtask 2.1. Define interface and instrumentation components required for utilization of the sample analysis chip.

The concept design for an adapter device for holding microfluidic and nanofluidic chips was developed with a specific size to be incorporated in the holder of the Vibratess' THz stage without requirements for extensive stage modifications, and at the same time able to accommodate different geometries of periodic micro/nanofluidic channels with inlet and outlet channels as needed. This provided flexibility to the spectrometer with modifications only to the adapter device- fluidic system.

A fluidic chip holder has been designed and fabricated (Figure 2-1). The bottom piece of the holder contains a small aperture for transmission of the THz radiation only through the patterned area of the array. The top piece of the holder keeps the device in place and provides the fluidic connections to the device. To allow for filling of the devices with liquid samples, a special manifold, made of polycarbonate Lexan, was fabricated to connect off-the-shelf tubing to the fluidic chip. This manifold, shown in Figure 2-2, also served the dual purpose of clamping one side of the flexible fluidic chip to the rigid metal base (Figure 2-1). The manifold accepted four tubes, three inlet ports and one outlet port, with two small screws threading through the manifold and into the metal base. The area around each of the four fluid ports is sealed using a small rubber O-ring. On the opposite side from the manifold, the fluidic chip is clamped to the metal base using two more screws through a small Lexan bar of the same dimensions as the manifold.

Once assembled on the holder, the fluidic chip is much more rigid and dimensionally stable for the scanning process (Figure 2-3)

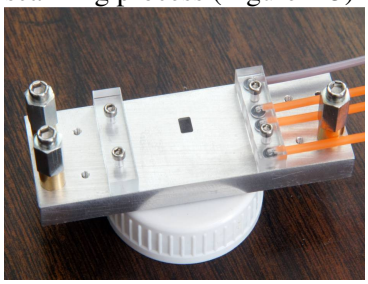

Figure 2-1. Fluidic chip-holder with the apperture for THz radiati

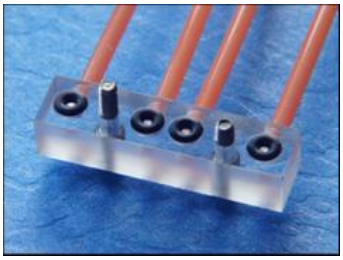

Figure 2-2,.Fluidic chip manifold

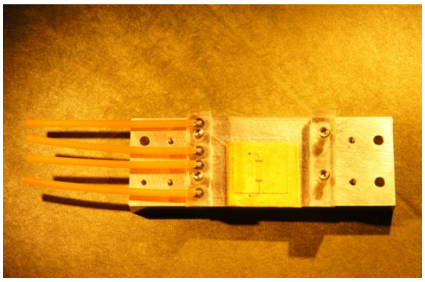

Figure 2-3. Chip-holder with a fluidic chip device placed above the aperture.

To utilize this interface to move liquid through the sample analysis chip, syringes could be attached to the tubing at each inlet position, and each syringe controlled by a syringe pump. Syringe pumps with pL flow rates were identified and ordered, and tubing, syringes, and the necessary fittings were obtained from Upchurch Scientific. For the initial testing, however, a syringe pump was connected with the tubing at

the outlet position in the device holder manifold as shown in Figure 2-4. This arrangement allowed liquid to be pulled into the chip, creating less pressure on the cover layer, and preventing delamination of the cover from the array. For the current work, an alternative method has also been developed and the necessary components fabricated, in which open reservoirs replace the tubes on the inlet ports, each having a screw valve which is used to control the flow of material from each reservoir. Figure 2-5 shows a chip in the holder with this new manifold, with a different color solution in each of the three reservoirs and associated inlet channels in the device. Using the withdrawal mode on the syringe pump and sequentially opening the valves on the manifold, each of the three color solutions was pulled through the device.

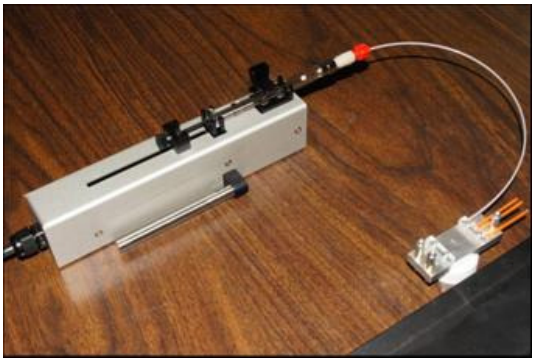

Figure 2-4. Syringe pump connect with the chip holder.

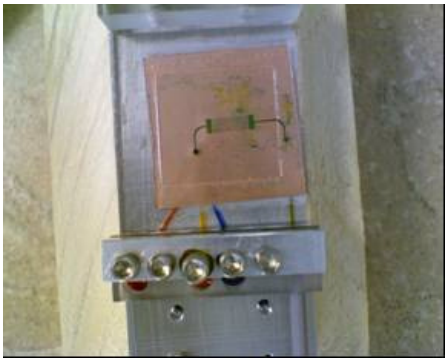

Figure 2-5. Manifold with inlet reservoirs using valves to control flow from each inlet.

The system for circulating liquid through the arrays was integrated into the spectrometer system. This entailed mounting the syringe pumps onto a platform on the instrument designed for this purpose and modifying the tubing/connectors to fit the implemented system. Figure 2-6 shows a single syringe pump mounted on the spectrometer system. (Note that the mounting plate will accommodate two syringe pumps at the same time, but only one is shown to allow better visualization of the syringe and its tubing connections). At last Figure 2-7 demonstrates the single syringe pump microfluidic system integrated with the spectrometer. The brackets on the plate allow for easy installation and removal of the pumps, as well as lateral adjustment of the pumps' positions when connecting the stiff tubing. Each syringe pump has its own external control box that allows the user to program the volume of fluid to be injected or withdrawn by a syringe, and the delivery/removal rate. This option allows users of other spectrometers to implement the flow control system into their instrumentation with the appropriate mounting of the holder and syringe pumps.

For our system, control software for the syringe pumps was directly incorporated into the software used to control the spectrometer itself. This software provides all of the same control setting including infusion or withdrawal modes, and rate and time controls. Both the control boxes and our software allow for additional programming, such that the syringe can be withdrawn a certain volume to generate a vacuum, and held for a certain period, before being returned to a set position to reduce the vacuum and stop flow into the array.

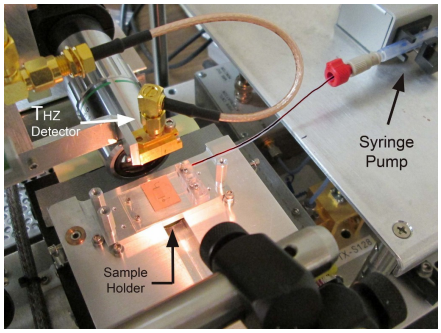

Figure 2-6. The flow system as mounted i spectrometer: a microfluidic sample analysis device in the holder is mounted in the detection region of the spectrometer, and connected with the syringe pump to control fluid flow.

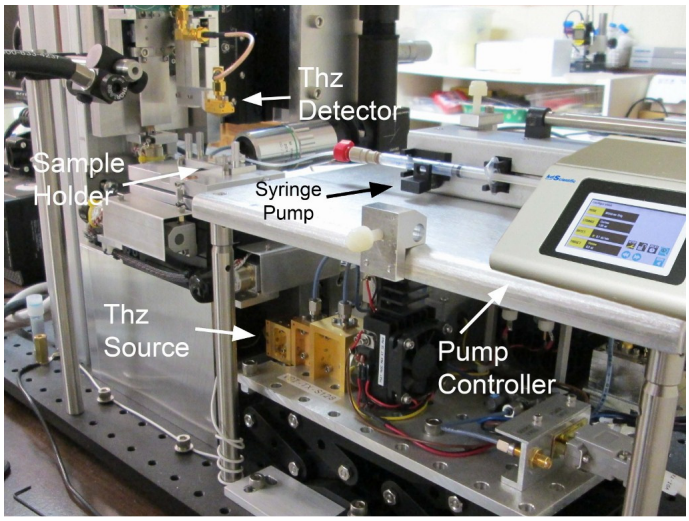

Figure 2-7. Microfluidic system utilizing one syringe pump is integrated with spectrometer.

Subtask 2.2 Flow control: pressure driven flow

Initial testing of the system for introduction of a liquid sample into the arrays focused on flow control using pressure/vacuum driven flow. A syringe attached to the outlet tubing of the chip holder (Figure 2-4) was put into a syringe pump and tested in both infusion (pressure) and withdrawal (vacuum) modes. With the initial cover layer bonding technology, pressure-driven flow caused delamination of the cover due to minimal adhesion of the thin adhesive layer. A syringe attached to the outlet port with the syringe pump operating in withdrawal mode allows fluid to be pulled through the channels without delamination of the cover. This method allowed individual fluids to be pulled in from each of the three inlet reservoirs when utilized with the valved manifold described in Task 2.1.

Use of vacuum to pull liquids into the array allows us to pull multiple solutions through the array, but does not provide good control of flow. While initial use of pressure driven flow was not possible, the implementation of the newest ADCOTE adhesive formulation for bonding cover layers did allow pressure driven flow to be performed. Flow rates of 10 uL /min easily generated movement through the array, which could be visualized using color solutions. Pressure driven flow is now routine through these devices.

Subtask 2.3 Flow control: electrokinetic movement

In addition to flow of materials using pressure driven flow, the use of electrophoretic movement of molecules into the array was investigated. To utilize electrophoretic flow, the microfluidic device first had to be filled with a buffer solution that would support a flow of ions through the system. In addition, electrodes were needed at the inlet and outlet ports for the application of the potential which would drive the electrophoretic movement of molecules. The reservoir manifold shown in Figure 2-4 was modified to permanently incorporate a steel electrode on the outlet side where the tubing connect into the manifold. For the inlet electrode, a piece of platinum wire was placed into the inlet reservoir which was filled with liquid for testing. The resistance between the two electrodes was measured while liquid was pulled into the array using a syringe to create a vacuum - a measurable resistance indicated liquid filling the channels in the device.

While liquid did fill the array, a stable resistance was not obtained. This was determined to be due to the small amount of liquid in contact with the outlet electrode. Liquid reaching the outlet electrode tends to flow past the electrode and into the tubing and syringe, which does not provide a good connection with the electrode. To eliminate this problem, the syringe was instead filled with the buffer solution being used, and buffer was pushed into the device from the outlet using the syringe pump. This filled the outlet area around the electrode and allowed for good contact between the solution and outlet electrode. A measurable resistance could consistently be obtained between the inlet and outlet of each device.

For electrophoretic testing, a voltage was applied between the inlet and outlet electrodes, and a stable current in the microamp range was achieved through the devices. This current flow through the device indicates that electrophoretic movement is occurring through the devices for the charged molecules carrying the current. While performing the electrophoretic experiments, however, it was noted that the current decreased with time, and could be regenerated by flowing additional material into the device. The most stable currents were achieved with continued pressure driven flow of material through the device during voltage application. This again seems to be due to the small volume of liquid in contact with the outlet electrode. Electrolysis taking place at this electrode during the course of the experiment is displacing the liquid surrounding the electrode, leading to reduced currents.

Conclusions for Task 2

In this project, we have developed the necessary holders and control system to allow flow through a microfluidic sample analysis chip while it is mounted within the detection area of the THz spectrometer. The holder was designed to provide flexibility in the design of the microfluidic chips and potential array designs, and to be mountable in other commercially available spectrometer systems with little modification. The system for generating flow through the chip utilizes commercially available pumps, which are controlled directly by the spectrometer software in our system, but can be controlled through the commercially supplied controllers for use in other spectroscopic systems.

Flow through the sample analysis devices using this system is possible using both infusion and withdrawal modes, to either push liquid into or pull liquid through the array. Improvements in the devices were required to achieve good pressure driven flow, but these have been completed. Electrophoretic flow of ions through the system was shown by the generation of a stable current through the system, but additional modifications are needed to the manifold to allow for good contact with the outlet electrode during the electrophoretic movement investigations.

III. Development of interface packaging fluidic platform with THz spectroscopic system and required system modifications (Objective III).

Spectroscopic system modifications included new components design and fabrication, as well as modified system assembly. The new system also included development of a new data acquisition sub-system. All modifications and improvements were tested and evaluated.

Subtask 3.1 Modification of the Sample Holder.

A modified sample holder was described in Section II (Subtask 2.1). It is shown in Figure III-1 together with a disposable fluidic chip. A chip in a thick back frame, disassembled from a holder, is shown on the right side of the Figure 3-1. To assemble the construction a back frame is attached to metal base (on the left), the array being faced the rectangular hole in the base.

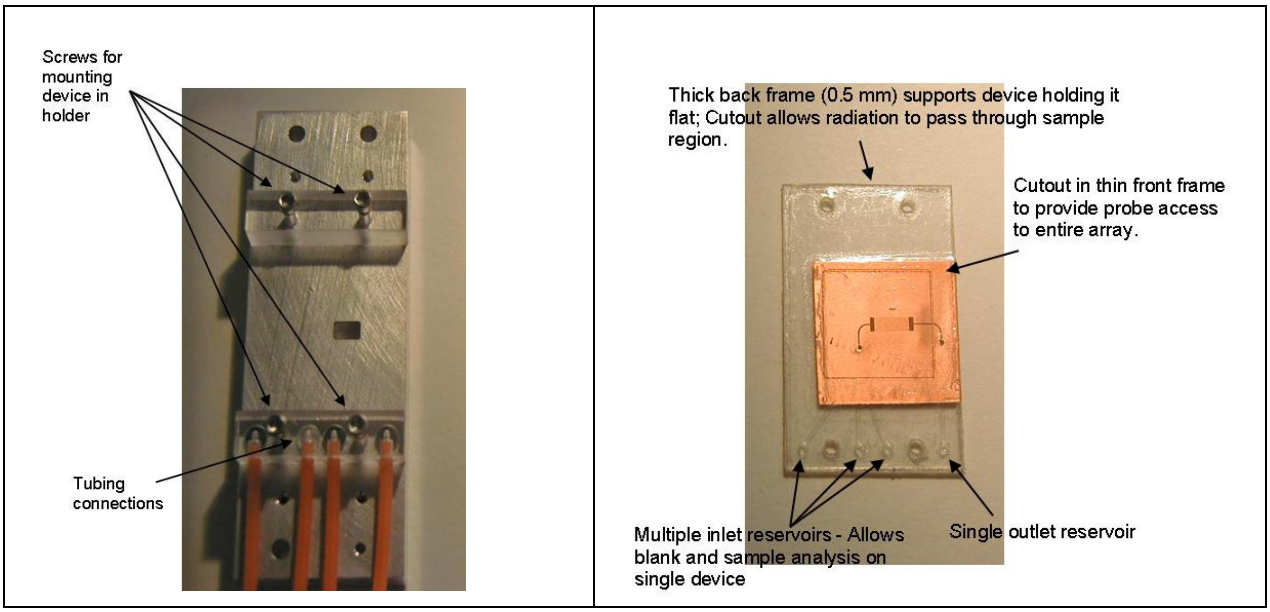

Figure 3-1. A modified sample holder (left) and a disposable fluidic chip (right).

Subtask 3.2 Automated height (Z-axis) positioning of the probe

One time-consuming task in the Phase I research has been the manual height adjustment of the probe during the initial sample set-up and subsequent repetitive scanning processes. To speed up the entire sample analysis process, in Phase II we incorporated automatic height adjustment of the probe into the spectroscopy system (currently, all three of these axes are adjusted manually using precision micrometers). An important improvement to the probe's linear positioning stage is a new feature that allows fast initial positioning of the THz probe. The precise linear stage is now mounted on a second slide that allows manual movement of the probe about one inch and position lock using a handle (Figure 3-2). This allows the samples to be changed without having to wait the long time otherwise required for the high-resolution stage to move the probe out of the way. Experimental evaluation has shown that it allows extremely accurate reproducibility (better then ~ 25um in all three coordinates) of the detector system's repositioning to a working location close to a sample microchip holder (at the bottom of the Figure 3-2) in a near field sensor configuration. This new feature will significantly reduce the overall set-up time for each sample when it is placed on the system for characterization.

Subtask 3.3 Modification of a microdetector housing

Previously, THz probe only allowed scanning with the sensing tip at an orthogonal orientation relative to the scanned surface. However, to better access covered microfluidic channels with a THz probe, a microdetector housing is being developed that should allow the probe's sensing tip to approach the fluidic chip at a significant angle (see Figure 3-3). A variable angle of as much as 50 degrees from vertical appears possible. This has been made feasible by significantly shrinking the probe's size in one dimension and increasing the housing's angle leading to the tip. Instead of consisting of two similar "halves" as in earlier designs, the housing now has a large "bottom" that completely surrounds a much smaller "top". As before, these parts are fastened together using small screws. However, because the "bottom" now surrounds the "top" on three sides, there is no longer a need for locating pins to register the mating parts. **A new and smaller version of a microdetector housing,** to be combined with a micro-fluidic platform, has been designed, fabricated, and delivered by Winchester Tool. This housing (Figure 3-4) is not only smaller, but much more robust and convenient for installing in it a microdetector with a probe and a microcircuit.

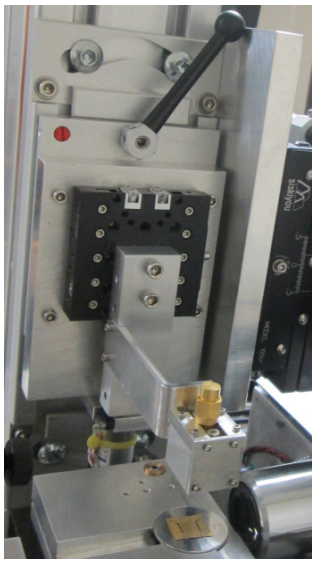

Figure 3-2. Precise linear stage with an extremely accurate and reproducible manual movement

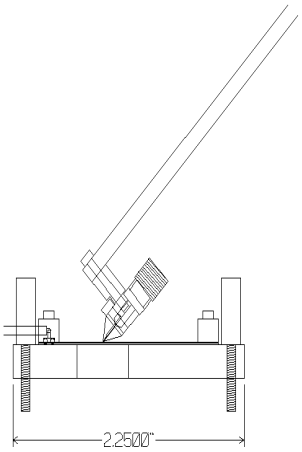

Figure 3-3. The design of a holder assembly with an angled probe housing. Variable angle is possible.

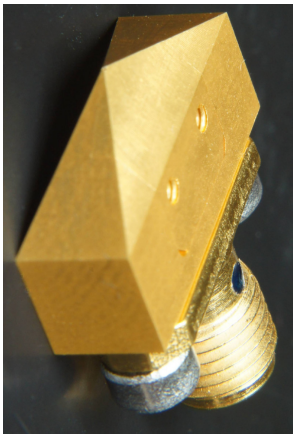

Figure 3-4. A small housing with an SMU connector for assembling a microdetector with a circuit and a probe.

Subtask 3.4. A new data acquisition system and software.

One of the most important aspects of this project is developing completely new data acquisition sub-system with the goal of an accurate signal registration. We researched the possibility of using new hardware to simplify and optimize the performance of the existing spectroscopic system. With the help of our consultant from the UVA, Dr. Harry Powell, the USB 6281 multifunction module from National Instruments was selected and purchased. A bloc diagram for a spectroscopic instrument with a new data acquisition subsystem utilizing NI USB module is shown in Figure 3-5. Note that the items depicted with dashed lines would only be utilized during periodic frequency calibration of the spectroscopic system.

The USB 6281 was supplied with the standard NIDAQmx 9.3.5.1 driver files, and a new dynamic link library (DLL) file was created to allow the instrument to be integrated with our spectroscopic system. A test application was created that allowed us to evaluate the performance of the new USB device with our spectroscopic system. Tests showed that the system worked as we expected. Figures 3-6 and 3-7 compare the previously used data acquisition system with the new one. All standard, bulky and expensive electronic devices, including the lock-in amplifier, two power supplies, and a frequency meter shown in Figure 3-6 are replaced by the NI USB device and controlled by a revised software application. This approach not only reduces the size, weight, and cost of a spectroscopic sensor system, but it also improves the system performance and simplifies it use.

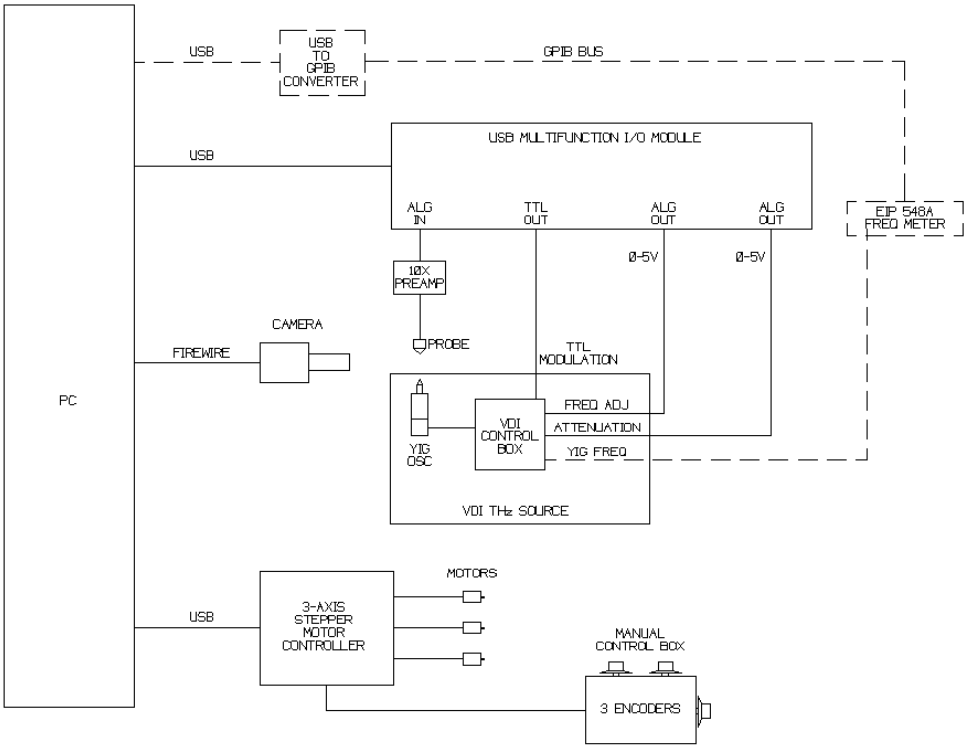

Figure 3-5. Block diagram for THz Spectroscopic Instrument utilizing a NI USB device for a new data acquisition sub-system.

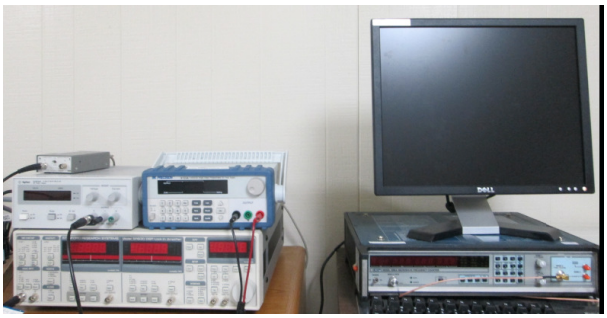

Figure 3-6. The previously existing data acquisition system that includes: Lock-in-Amplifier, two power supplies, preamplifier (on the top), and a frequency meter (under a computer monitor)

Figure 3-7. The USB 628 from National Instrument (note an enlarged scale compared to a Figure 3-6). The computer and monitor are the same as in the existing system (not shown).

At the same time, the previously existing software that was used for the spectrometer operation and for data collection has been modified to allow it to be used with the new USB device. A new custom-designed preamplifier circuit, was designed by our consultant Dr. Harry Powell (Figure 3-8) to substitute the original lock-in amplifier's preamp. Preamplifier was assembled onto a circuit board (Figure 3-9).

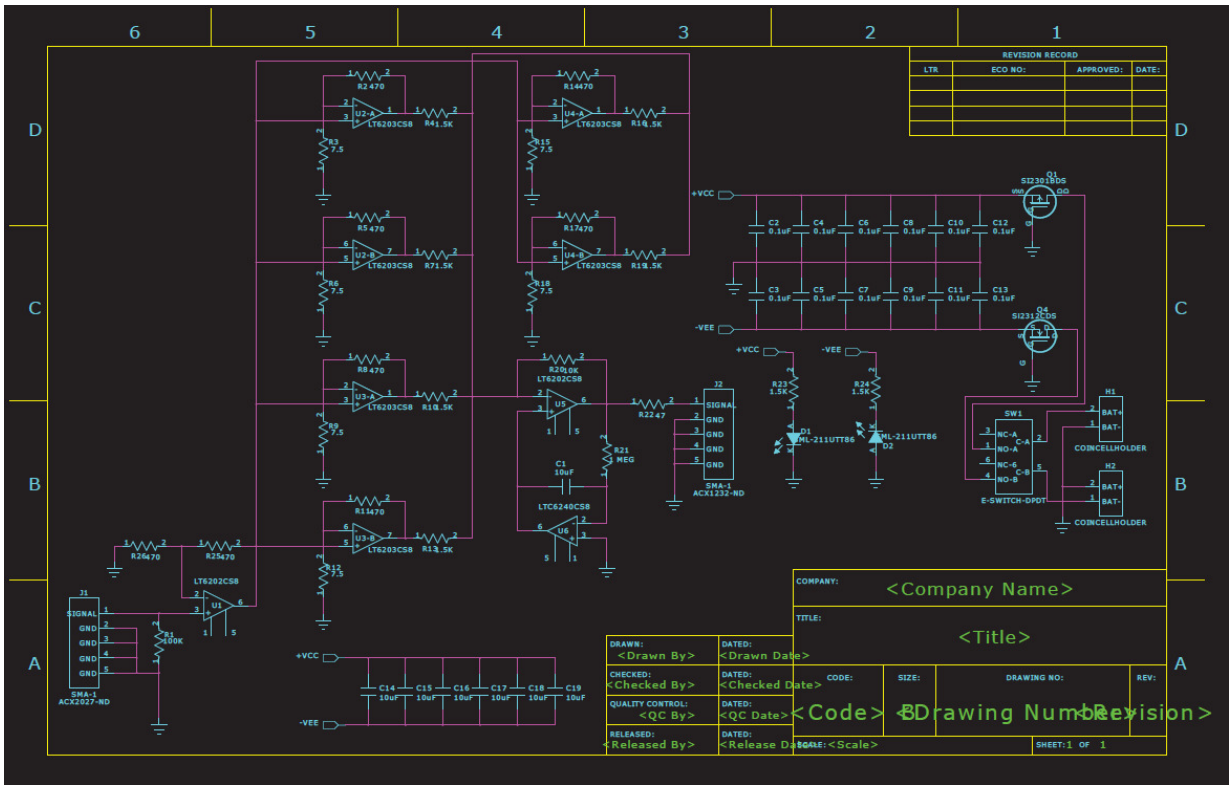

Figure 3-8. Preamplifier board-circuit by Dr. Harry Powell, Version 1.

As part of a new data acquisition system, this new board allows the elimination the old preamplifier that was used to make measurements of the THz signal. Due to its smaller size, a circuit board is connected directly to a microdetector housing thus also eliminating the use of long cables. Additionally, it is powered by batteries. to reduce its noise. All these improvements lead to reduced noise in the data acquisition system. The circuit board is mounted on a supporting plate that was designed, fabricated and installed on the spectroscopic system. Note that the detector (probe) housing also mounts to this new plate, thus creating a more robust and mechanically stable microdetector sub-system (Figure 3.10).

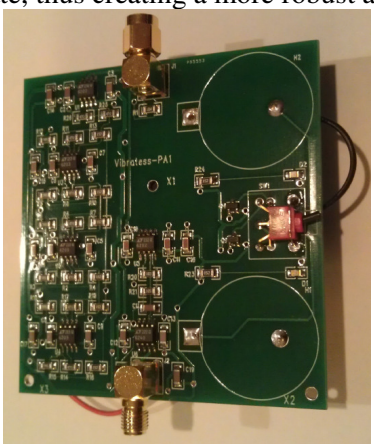

Figure 3.9. A custom preamplifier circuit board. Two circles show the place for batteries

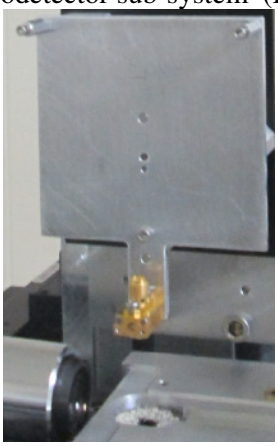

Figure 3.10. The baseplate shown above is used to support the new preamplifier circuit board. The probe housing also mounts to the bottom of this new plate.

The board is now fully functional and, along with the USB multifunction module, is being used to evaluate the overall system performance without the need for the original instruments. It has been tested, and the results confirm its operation with the expected voltage gain of 1750. Experiments have been conducted to find the best parameter values that will achieve an adequate S/N ratio while still minimizing the measurement time. The results of our experiments appear to indicate that averaging of 133,000 data samples is our best option. However, the intrinsic noise of the preamp was initially higher than the noise of our microdetector and the signal to noise ratio was restricted by the intrinsic noise of the preamplifier.

In our previous data acquisition system, we had a rather good signal to noise (S/N) ratio due to the Lock-in Amplifier's narrow bandwidth of ~0.01 Hz. However, the disadvantage of this prior approach, apart from the use of several costly and bulky electronic instruments, was the requirement for a long signal measurement time. We had experimentally determined that a delay time of at least 3 sec was required for an accurate signal measurement at each frequency point (frequency domain without averaging). The data acquisition module from National Instrument (NI) has an option to include a low pass filter for the measured analog signal. The 3-db cutoff frequency for this filter is 40 KHz compared to 450 KHz without a filter. Our initially produced DLL installation software was updated to implement all available software functionality, allowing control of the input filter defined by the manufacturer. The spectroscopic system's control software was modified to implement these options when making measurements using our THz detector. Using the filter resulted in a four-fold improvement of the signal-to noise ratio.

In order to be able to quickly obtain a signal/noise performance roughly equivalent to the previous data acquisition system, we are now using a Fast Fourier transform (FFT) procedure. This permits us to use software processing of the detector signal to quickly obtain a valid measurement, while still maximizing the S/N ratio electronically. To achieve this goal, the existing software was significantly modified to include the ability to capture a large number of voltage samples of the signal and store these in an array that represents the signal in the time domain. From this array, a software FFT routine produces a second array that represents the signal in the frequency domain. Other new capabilities have been added to the spectrometer's operation software to enable the capture and display of both the time-domain and fast Fourier transform (FFT) information obtained when making measurements using our THz micro-detectors. Newly enhanced software functionality include testing that provided graphical frequency and time domain presentations that allowed us to determine the system signal amplification and signal/noise ratio over the entire THz frequency spectrum supported by our sources. This latest innovation significantly facilitates the diagnostic process to evaluate and eliminate excessive noise in the system and enable us to more easily improve the system performance. Final debugging of all software modifications and enhancements has been completed.

Experiments have been conducted to verify the new approach and to test the parameter values that will achieve an adequate S/N ratio while still minimizing the measurement time. The maximum sampling rate of the USB 6281 module from National Instruments that we are using is ~500,000 samples/s. This permits us significantly reduce measurement time for one reading. The following three figures demonstrate the potential to improve the S/N ratio using FFT procedure. Figure 3-11 shows signal and noise as registered in time domain. TTL digital modulation, available from the USB device, is used with a period of 500 Hz. In the example shown in Figure 3-11, the signal is close to the noise level. The following Figure 3-12 demonstrates graph of the FFT signal in the frequency domain and clearly shows the first four harmonics, together with the noise on the bottom of the graph. Figure 3-13 is an expanded portion of the same graph showing only the first harmonic.

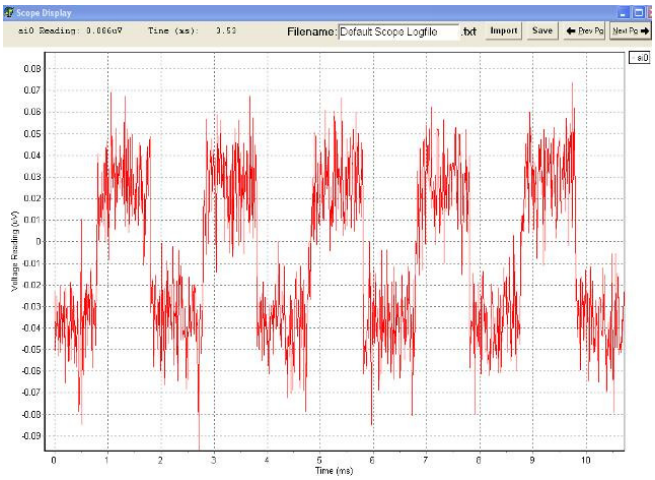

Figure 3-11. Signal and noise in time-domain using USB 6281 module.

The interface software has been prepared for our spectrometer with a new data acquisition system. It has been successfully used for data collection and analysis in all tests conducted on a new spectroscopic sensor to verify all modifications and improvements. Experiments have also been conducted to determine the required adjustments of the positioning of optical and mechanical components, including mirrors, THz sources, and detectors. These functions have been identified as being crucial in system assembling procedures.

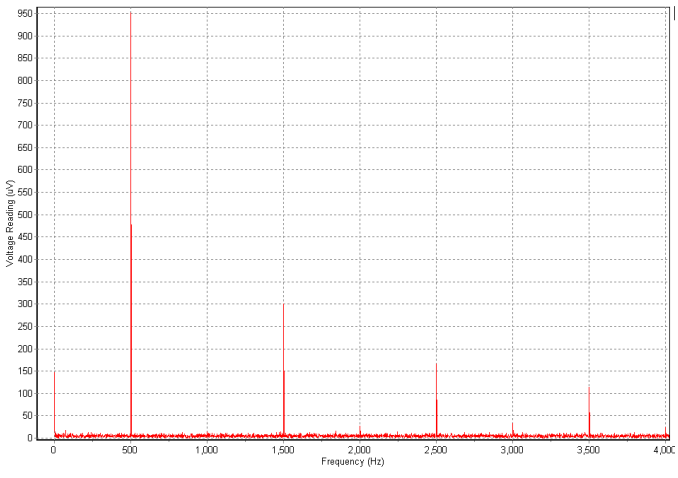

Figure .3.12. Signal in frequency domain (Fast Fourier Transform – four harmonics).

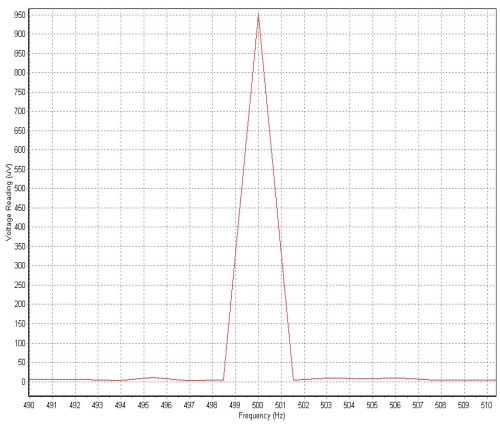

Figure 3.13. Signal in frequency domain (Fast Fourier Transform - first harmonic)

To facilitate operator training, an "Operational Manual" for a modified spectroscopic system has also been written (See Attachment #1 to Q5 Report: "Operational Manual for a THz Spectrometer with a NI Data Acquisition System", July 2013).

Subtask 3.5. Assembling a modified spectroscopic sensor system.

A modified spectroscopic sensor system has been assembled. The system includes all linear positioning stages and their motors, a motor controller board, a new optical mirror mounting system, a

power supply, a THz source, and a detector sub-system. All wiring and assembly have been completed (Figure 3-14, see also Figure 2-7)).

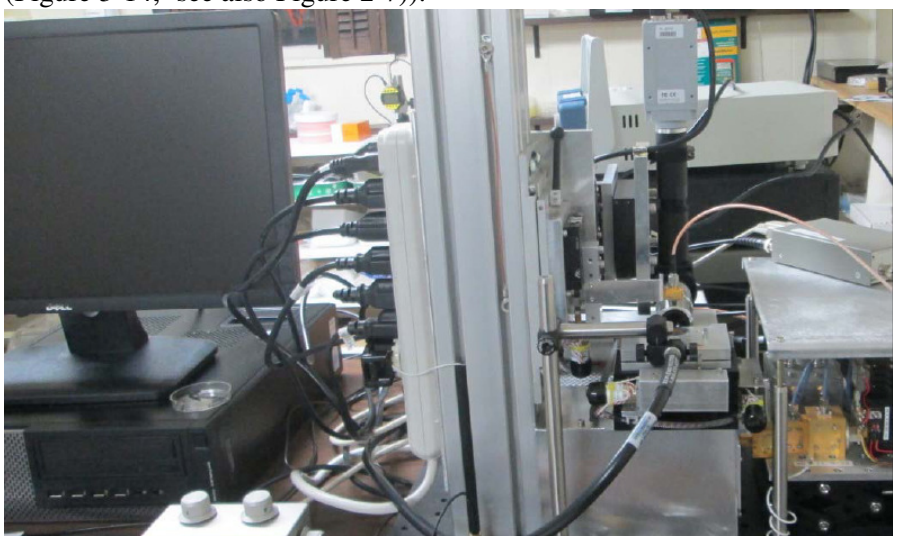

Figure 3-14. A modified spectroscopic sensor system

IV. System testing and evaluation (Objective IV).

Subtask 4-1. Testing devices quality in spectrometer set-up

The previously developed by Vibratess spectrometer prototype operating with high spectral and spatial resolution described in [2] was used for testing quality of newly developed devices and components. This instrument that was built in 2008 and intensively used for more than 4 years for biological material characterization required periodical adjustment and repairing. Additionally an optical experimental set-up was assembled for testing THz sources and detectors used in our spectroscopic systems. The tests showed that the old THz source has been damaged in the multiple experiments with new acquisition system development. It was repaired by VDI, reinstalled in the system and spatially adjusted using new clamping mechanisms. The repaired instrument was further used to characterize components in multiple experiments.

Using this spectrometer all constructive materials for substrates, adhesives, and cover layers to be used in our new technology for microfluidic chips has been tested. One of the goals of these experiments was the complete evaluation of the reproducibility of geometry and performance of microfluidic chips that are easy to fabricate. Testing experiments on all components used in technology development demonstrated very good optical transmission and hydrophilic surface, both attributes being absolutely necessary conditions for a good performance. The problem has been, however, identified that was related to use of DuPont Pyralux**-** polyimide sheet with 5 μm thick copper layers laminated to both sides (***Subtask 1.1)***. As demonstrated in Figures 4-1(a) and 4-1(b) that technology does not provide reproducible width of channels, and the channels side walls are not smooth due to striations and grain structure in the original copper layer laminated onto the polyimide. These defects reduce the reproducibilityof probe positioning at the channel edge to approximately 2-3 μm, thus reducing the compatibility of background and sample measurements and limiting the overall accuracy of biological sample transmission measurement to not better than 3-5%. It is also difficult to produce channel width less than 12-15 μm, although optimal channel width for microchips is 10 μm at our frequencies, and would be much smaller for nanofluidic chips.

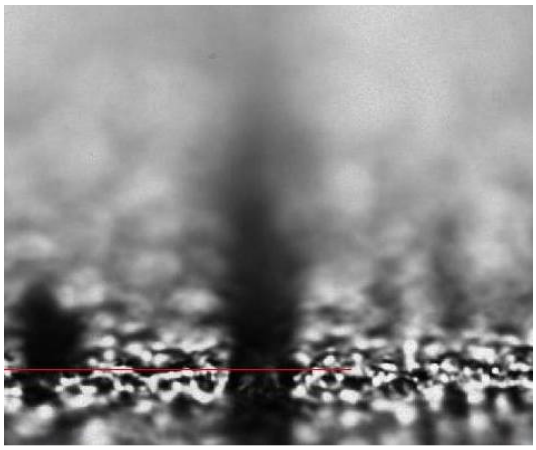

Figure 4-1(a). Grooves are parallel to channels (vertical orientation in the image). Horizontal pattern is a boundary between a chip substrate surface and it reflection in a metal base.

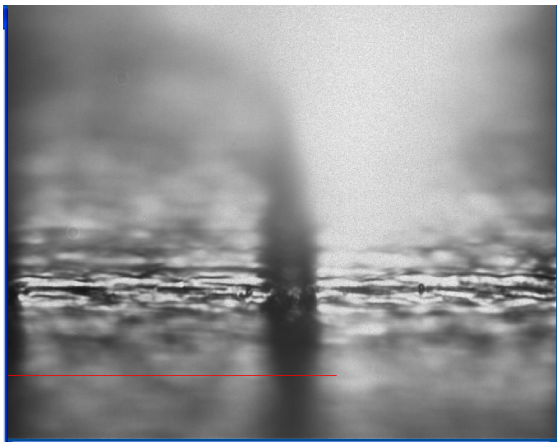

Figure 4-1(b). Grooves (horizontal) are perpendicular to channels (vertical).

New fabricated microfluidic chips are currently used for characterization of biological materials. Testing includes reproducibility of results from material in different channels as well as at different positions along the channel.

Subtask 4-2. System testing and evaluation. Spectroscopic characterization of biological materials using fluidic chips.

Other possible reasons for some inconsistent measurements have been studied as well, including instabilities of sources, detectors, and poor reproducibility of a probe mechanical positioning. It was found that mechanical positioning is highly reproducible providing an accuracy of transmission within 2%. The source was also found to be stable, being within 2% during the entire day of work, although each new source must be tested. The stability of detectors depends in much degree on quality of assembling within a housing, and each new detector has to be tested as well.

The serious problem that has been identified is a broad variation of microdetectors' spectral responses. One of possible explanations is our identification of a technology change in the fabrication of Schottky diodes by VDI, the diode manufacturer. We have recently observed during our assembly process and in our experiments that the size of elements and the thickness of substrate has been reduced, and the technology has been modified resulting in changies to the current –voltage characteristic, zero bias resistance, capacitance and other parameters. These changes, however, can perhaps be used to our advantage in possible expanding the spectral range of sensitivity to higher frequency with corresponding adjustment of our circuit characteristics in future projects.

Working on another problem, we conducted extensive experimental testing of the accuracy of spectroscopic characterization of biological samples in the system prototype with microfluidic devices currently under development. One of the most important factors that might influence the accuracy is the reproducibility of detector micro-probe positioning over the sample material in the microfluidic chip cannels. To test the system sensitivity for possible inaccuracy in positioning of the tip of the detector, several background scans were run on the same structure but with tip positions artificially varied by 1-2 □m in X and Y directions, and the normalized root mean square (RMS) deviations from the averaged spectra were calculated. Figure 4-2

demonstrates high reproducibility of three background spectra measured at three different Y coordinates along one channel with the step of 1 um. Although very big variations for radiation intensities are observed depending on frequency, very high stability of all components including the THz source, together with accurate voltage values, which control the THz source's supplied frequency, provide a low level of error and high reproducibility in signal and transmission measurements. RMS deviations for these three background spectra shown in Figure 4-3 (black plot) indicate very small error values within 1-3 % over the frequency range of 11.6-16.8 cm^{-1}. Rare "spikes", where differences exceed 1% limits, are due to very low absolute signal strength at these frequencies as shown in Figure 4-2. Slightly bigger values of RMS error were obtained for the shift of the probe position in the direction across the channel (X-coordinate), as demonstrated by a green curve in Figure 4-3.

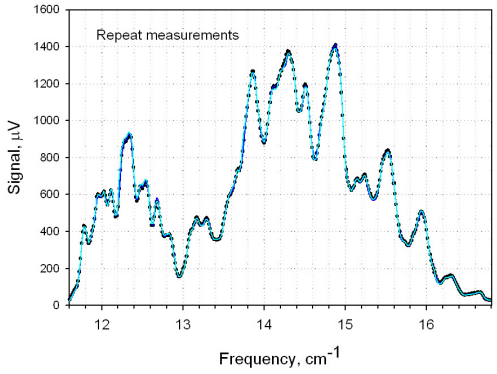

Figure 4-2. Reproducibility of three background measurements at slightly different position of a probe (2 μm) along the same channel.

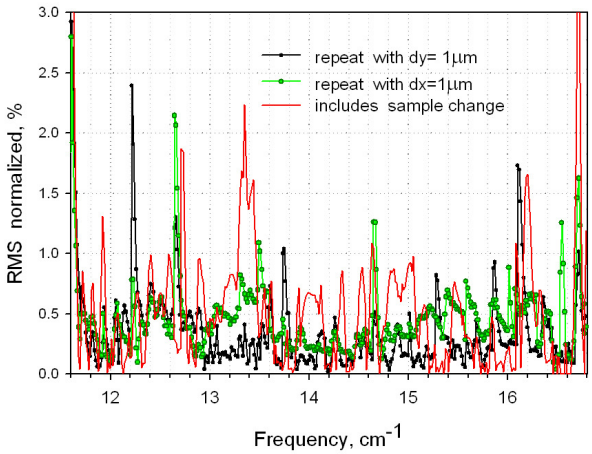

Figure 4-3. RMS deviation from the average in three situations: 1-measured with a 1um shift along the channel of a probe relative to the microchannel with sample material (black); 2- same with a one micron shift in the direction across the channel (green); 3-movement of a microprobe and detector at a large distance between measurements, including adding new sample material (red).

Finally, the results of two transmission spectra measurements for ovarian cancer cells material with low concentration of 100 cells/μl in solution and a small volume of solution (0.3μl), as shown in Figure 4-4, were used to calculate the RMS deviation in the case where removal and replacement of the sample might contribute to the error (red curve in Figure 4-4). A low concentration of sample material in this case resulted in a low probability of getting a cell in the field of view of the. microprobe, thus explaining why the scaling in transmission is not observed after the second drop of material is added.

We expect that the exact positioning of the sample material under the probe in a new spectroscopic system combined with a microfluidic platform will significantly simplify the current procedure of material characterization and further improve the sensitivity.

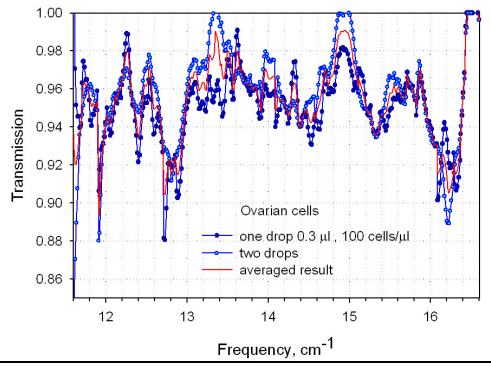

Figure 4-4. Two transmission measurement results for ovarian cells material with low concentration of 100 cells/ul in solution and small volume of solution (0.3 ul) resulted in a low probability of getting a cell in the field of view of the microprobe. The error in transmission measurements includes the contribution due to replacement of the sample

Subtask 4.3. Theoretical and modeling work to improve the efficiency of covered nanofluidic chips grating (consultant Prof. B. Gelmont)

This sub-task will include further investigation and characterization of the proposed grating structure with the goal to improve the efficiency for enhance coupling of THz radiation with biomaterials under test inside the covered nanofluidic chip. The theory was developeing by the consultant B. Gelmont

Theoretical evaluation of transmission of nanofluidic chips.

The transmission of nanofluidic chips was calculated depending on the channel widths between 20 nm and 10 µm, and the spacing between channels up to 250 µm. Reasonable transmission of ~ 40% can be achieved even with very narrow channels of only 20 nm width for periodicity of ~ 100 µm (see Figure 4-5). The thickness of channels (gold) was not included in this analysis. A 3D graph in Figure 4-6 demonstrates the transmission of an array of channels at the frequency of 15 cm^{-1} depending on channels width and periodicity. The information was used for the nanofluidic chip design.

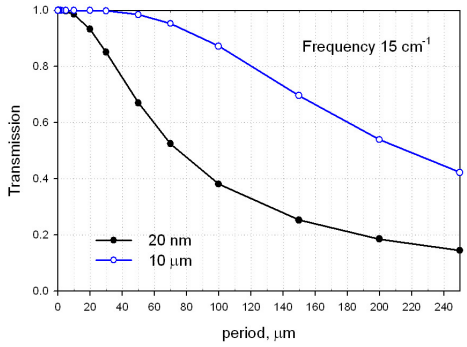

Figure .4-5 Comparison between transmission of arrays with the channels of 10 □m and 20 nm depending on channel periodicity in array.

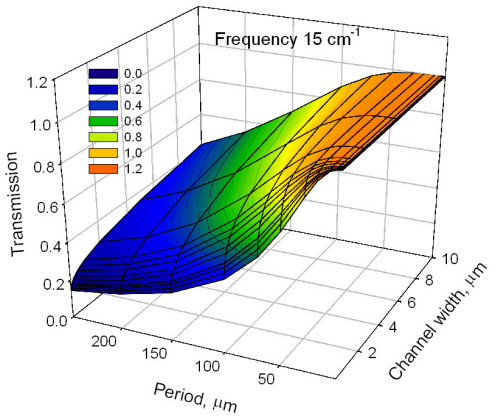

Figure 4-6. Transmission of nano-channel arrays depending on channels width and period.

Transmission of periodic lattice having finite thickness.

The earlier evaluation was only performed in the limit of a zero conductor (metal) thickness. The issue of being able to transmit THz radiation through microfluidic chips built with several layers, all having finite thickness, is now becoming important. The transmission through the conductive lattice with a finite

thickness is determined as a function of frequency for the period of the lattice and its thickness both smaller than the wavelength of radiation. Derived basic integral equations have a singular kernel. An algorithm has been developed for the solution of such equations determining transmitted electromagnetic field through a conductive lattice having finite thickness and the results of an analysis for two sets of grid geometrical dimensions is shown in Figure 4-7.

Array geometry optimization

Further analysis of various combinations of grid dimensions enabled us to determine a more optimum design that helps to improve the transmission of the THz radiation over the range of frequencies we use. The electric field strength can be characterized by the voltage across the slit. An algorithm has been developed for the solution of the integral equations determining transmitted electromagnetic field through a conductive lattice having finite thickness. This algorithm was utilized to find the optimal geometric parameters of the lattice. The electric field strength can be characterized by the voltage across the slit. As can be seen from Figure 4-8 there is an optimal periodicity L at a given width of the slit (2a=10 □m). This optimal periodicity required to maximize the voltage across the slit depending on the radiation wavelength, with higher values required for longer wavelength.

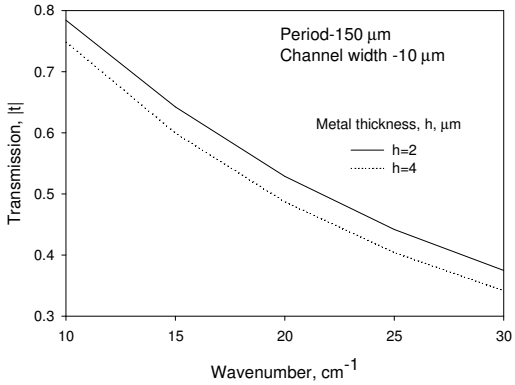

Figure 4-7. Far field transmission through microfluidic chips depending on frequency for two different thicknesses of gold layer, 2 and 4 um..

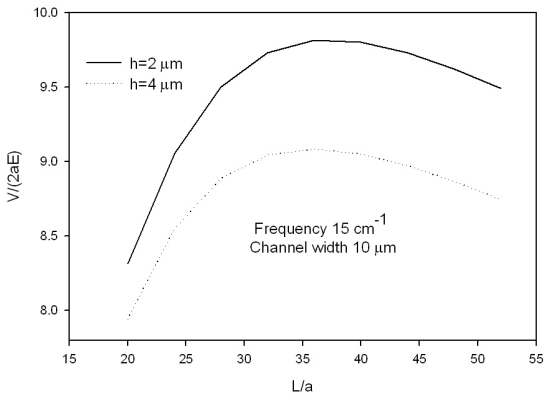

Figure 4-8**.** The optimal periodicity of an array, which maximizes the voltage across the slit, for two values of metal thickness, 2 and 4 microns

Subtask 4. 4. Protocol development for spectroscopic characterization of biomaterials using nanofluidics.

One of important tasks in this project (Task 4, Objective IV) is protocol development for spectroscopic characterization of biomaterials in solutions using micro/nanofluidic devices. Traditional analysis of the transmission of dry biomaterial in a thin layer, when the film dielectric permittivity is close to unity, shows that the transmission is determined mainly by the material absorption coefficient spectrum. For this case, the protocol to calculate the transmission and absorption coefficient from measurement results has been developed and verified earlier. The traditional approach can be used to calculate the transmission as a ratio of signal spectrum from radiation passed through the sample material in the channel of a device to the background signal measured without biomaterial. The resulting transmission in this case is always below 100%. However a new protocol has to be developed for quantitative spectroscopic characterization of biomaterials in water or other liquid solutions.

Imaginary and real parts of water dielectric permittivity in the sub-THz region are significantly higher then 1 and close to each other. As a result, the formal use of traditional protocol to calculate the biomaterial transmission using measurement results from water as a background gives artificial results

higher than 100%. Calculations of absorption have to be modified too. The corrections are significant and absolutely necessary in this case. Our consultant, Prof. B. Gelmont was working on development of a new approach to calculate transmission and absorption of biological materials in water or other solutions that is described below (See section V, subtask 5.1).

We have two options regarding to the protocol for spectroscopic characterization of biosamples in microfluidic chips.

1) Using a traditional approach. In this approach the frequency spectrum of radiation passed through a microfluidic chip without liquid is measured as a background, U(ch air), and the frequency spectrum of radiation passed through a microfluidic chip with biosample on solution, U(ch bio) represent the sample. Transmission of biomaterial in solution in this approach is calculated as a ratio of sample results to background of a dry channels

T (bio solution)= U(ch bio)/ U(ch air). A disadvantage of this approach is a probability of artifacts due to the fact that measurable amount of water in sample solution might change optical path of radiation relatively to background conditions of an empty channel. These artifacts are actually caused by a big difference in optical properties of air and water. The errors probability will be higher for diluted solutions.

2) Using a modified approach, in which the frequency spectrum of radiation passed through a microfluidic chip filled with pure water is measured as a background. In this approach, background and diluted solutions have very similar optical properties, and the probability of artifacts would be low. It however becomes more significant at high concentration of bio-material in solutions. Since characterization of small amount of bio-samples is usually a target and the most difficult to achieve, we have chosen the second approach. An additional advantage is that in this approach, the viscosity of bio-samples is less and filling of chips with sample materials is easier. Detecting of single cells and macro-molecules is a more realistic goal to be achieved in this approach too. For all these reasons, this second approach was used in experimental testing of bio-solution characterization using microfluidics, as well as in theoretical analysis to extract absorption spectra from transmission measurement results. (see next Section).

Spectroscopic characterization of biological materials in solutions (ObjectiveV)

In the Phase I we were able to characterize biological materials only in the solid state after drying in channels. We could not match sample and background spectra since channels were not covered and it was not possible to control the amount of liquid during measurements. With development of a new technology in Phase II we can now construct and cover the chips for characterization of biomaterials in solutions as part of this Objective. Construction of new chips with several inlets permits us to study and characterize biological and biomedical processes, performing measurements of signal which depend on frequencies (spectral characterization) and depend on time (kinetic of processes).

Subtask 5.1. Dielectric permittivity of water in the THz region. Designing microfluidic channels filled with water. Protocol development for THz spectroscopy (consultant Prof. B. Gelmont)

Till now we have characterized biological materials in their solid state. With the completion of a microfluidic system the measurements of sample materials in water solution is required. The absorption property of water depending on frequency is extremely important for an optimized design of microfluidic chips in the THz region. Water has strong absorption in sub-THz region and the losses of radiation due to water absorption have to be evaluated and taken into account. Our consultant, Dr. B. Gelmont, conducted a theoretical study to derive the equations and developed the software that can be further used for microfluidic chip design optimization and liquid sample materials measurements analysis.

Dielectric permittivity of water

The dielectric permittivity of the water is equal to 81 at zero frequency but drops to 1.33 at optical frequencies. Debye has shown how the static dielectric permittivity of the system of rigid dipoles can be calculated. The model developed by Debye has two parts. At first Debye has shown how the static dielectric permittivity of the system of rigid dipoles can be calculated. The dipole moment of water molecule, p, has been deduced from spectral characteristics of water vapor. In his first calculations Debye accepted

$$p(H_2O) = 1.87D$$

in order to describe the temperature dependence of the dielectric permittivity . The Debye equation for static dielectric permittivity is

$$\varepsilon_0 = \frac{4\pi N p^2}{3k_B T}.$$

However he underestimated the static dielectric permittivity ε_o of liquid water. The calculated static dielectric permittivity occurs to be 14 that is much less than the measured static dielectric permittivity, which can be approximated by equation

$$\varepsilon_0(\mathrm{T}) = 87.91\exp(-0.00458 * \mathrm{T°C})$$

Hence a picture of ensemble of noninteracting dipoles is too simple for water. A hydrogen bonded structure of liquid water is responsible for formation of four nearest neighbors that form a nearly regular tetrahedron with a given molecule at a center.

Kirkwood has shown how to correct the Debye theory taking into account the correlation in position of neighboring molecules. Utilizing the Kirkwood model, Frohlich derived the following equation for the static dielectric permittivity

$$\varepsilon_0 - \varepsilon_\infty = \frac{3\varepsilon_0}{2\varepsilon_0 + \varepsilon_\infty}\left(\frac{2+\varepsilon_\infty}{3}\right)^2 \frac{4\pi N p^2}{3k_B T} g,$$

where N is the dipole concentration, ε_ω is high frequency dielectric permittivity , Frohlich obtained the correlation parameter g=7/3 from the analysis of the geometry of the hydrogen bonded structure. The static dielectric permittivity was close to experimental value if the high frequency dielectric permittivity was taken as

$$\varepsilon_\infty = n^2.$$

It has been suggested (Hill 1963) that the dielectric properties of water at room temperature should be interpreted by taking the high frequency dielectric permittivity as the high-frequency limit of the Cole-Cole arc rather than the square of the optical refractive index. If this is done, the correlation parameter g has a value close to unity.

Dielectric permittivity of water in THz region

The second part of Debye analysis is related to the frequency dependence of the dielectric permittivity. He assumed that equilibrium is attained exponentially with time and introduced the constant relaxation time. Moreover he has shown how the relaxation time can be connected with the fluid viscosity η. In his treatment he considered an individual molecule as a sphere of a radius **a** moving in viscous fluid and obeying macroscopic equations of flow. Using Stokes's law he derived the relation between the relaxation time and the fluid viscosity η as follows

$$\tau = \frac{4\pi\eta a^3}{k_B T}$$

and has written an equation for the frequency dependent complex dielectric permittivity. Debye used macroscopic equations of liquid flow for estimation of the relaxation time. He considered an individual molecule as a sphere of a radius **a** moving in viscous fluid. He has taken a=1A and obtained τ=10 ps at room temperature. As a matter of fact, a radius of an individual molecule can be considered as an

adjustment parameter. It proved that such estimation of the relaxation time is a rather close to experimental parameters.

As a result the best way to approximate the frequency dependence of experimental complex dielectric permittivity is to write the Debye-like equation which contain three empirical parameters: the relaxation time, the static dielectric permittivity and the high frequency dielectric permittivity. In particular the empirical high frequency dielectric permittivity has to be taken 4, much larger than 1.33*1.33 taken by Debye and Frohlich. The relaxation time is taken 7,2 ps at 30 C (from the literature).

In standard treatment of biological molecules the imaginary part of the dielectric permittivity is small and the absorption coefficient is proportional to the imaginary part. However the imaginary part of the dielectric permittivity of water is comparable with the real part. Therefore a more complicated procedure is required for the determination of the absorption coefficient from the complex dielectric permittivity.

Debye has also developed the theory for frequency dependence of the complex dielectric permittivity. The frequency dependent dielectric permittivity can be found from the equation,

$$\varepsilon = \varepsilon_\infty + \frac{\varepsilon_0 - \varepsilon_\infty}{1 - i\omega\tau},$$

where ε_0 is the dielectric permittivity at static electric field, and ε_∞ is the high frequency dielectric permittivity. The dielectric permittivity of water has been modeled and compared with experimental data by Hill (Fig 5-1, blue curve).

Analysis of the transmission of thin films shows that the transmission is determined mainly by the absorption coefficient if the film dielectric permittivity is close to unity. Otherwise an additional multiplication factor, depending on the film dielectric permittivity has to be used. This correction is essential in the case of water.

Dr. Gelmont continued developing the theoretical model to calculate absorption spectrum of water and biosolutions and analysis of the correct relation between measured transmission and extracted dielectric properties (absorption coefficient and refractive index) of water.

The transmission of thin film is calculated using Hill's results.

New approach was developed and accurate equations have been derived to be used in experimental data analysis and used (see Subtask 5.2).

Following equations represent the relation between optical parameters and transmission (|t|^2)

$$|t|^2 = 1 - 4\,\mathrm{Im}(k_1 h \frac{1 + r_{12}^2}{1 - r_{12}^2}) + 4\,|k_1 h \frac{1 + r_{12}^2}{1 - r_{12}^2}|^2,$$

$$r_{12} = \frac{n + i\kappa - 1}{n + i\kappa + 1}, \quad k_1 = k_0(n + i\kappa), \text{ and } |t|^2 = 1 - 2h\alpha_{eff}$$

Broun curve in Figure 5-1 demonstrates effective absorption coefficient α_{eff}.

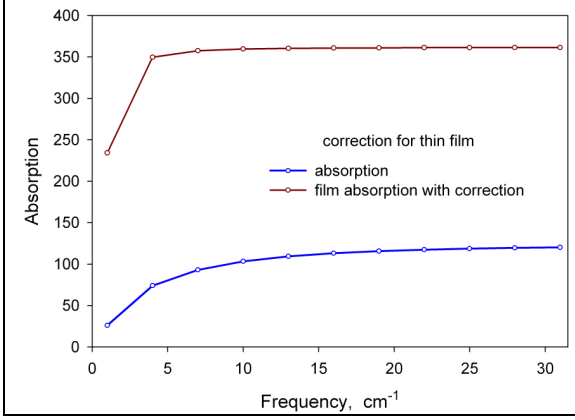

Figure 5-1. Modeling results for water absorption spectrum in sub-THz range.

These results have been used for microfluidic chip design optimization and liquid sample materials measurements analysis.

Subtask 5.2. **Experimental characterization of sub-THz transmission spectra from Herring DNA solution using microfluyidics.**

The experimental set-up has been described in the Subtask 2.1 of this Report (Figures 2-6 and 2-7). Microfluidic sample analysis device (chip) shown in Figures 1-19 has been mounted in the sample holder as shown in Figure 3-1. Pressure driven flow control was provided using a single syringe pump connected with a chip holder as it shown in Figures 2-4 and 2-6. The measurement protocol is described in "Operational Manual for a THz Spectrometer with a NI Data Acquisition System" (See Attachment #1 to Quarterly Report #5??). Regime of 133,000 data sampling points was used. A modified approach discussed in Subtask 4-4 was used to measure transmission. It means that at first the background spectrum was measured of the radiation pass through the fluidic chip filled with water using the syringe pump controller. After that a microdetector with a probe has been moved into the upper position using the mechanism shown in Figure 3-2, the water was substituted with solution of herring DNA using syringe pump controller (Figure 2-7), the probe was returned into the previous low position and the sample spectrum was measured using the same set of parameters.

Sample material of Herring DNA provided by research scientists from ECBC was used to prepare solutions in deionized water in two concentrations, 1 and 5 mg/ml, and the experiment was repeated for both sample concentrations. The same background spectrum was used to calculate transmission spectra for two samples. Sample scans have been repeated in two different channels of the chip.

Figure shows background spectrum of a chip with water and sample of H DNA spectrum. As it was expected, the signal from a chip with material is higher then from a chip with water.

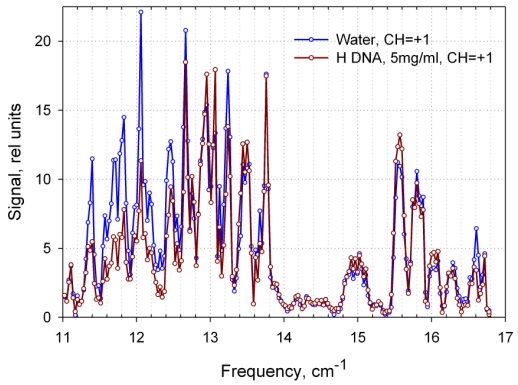

Figure 5-2. Background and bio-sample spectra

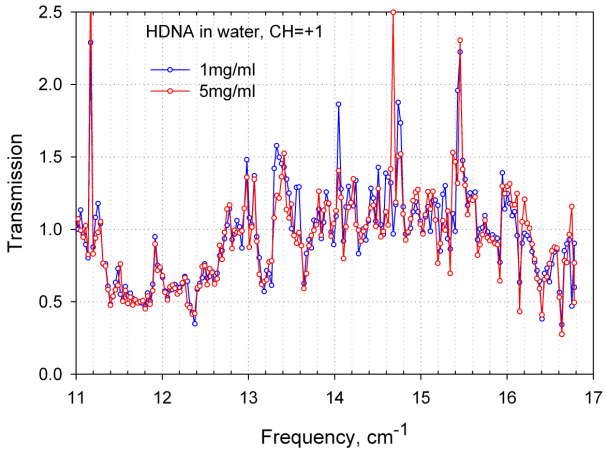

Figure 5-3. Transmission spectrum from H DNA

The background and sample spectra demonstrate very high variations of signal depending on frequency, which of course is not desired. The pattern is the result of multiple reflections and resonance phenomena that occur in the system. Nevertheless, transmission spectra calculated as a ratio of sample to water spectra give very reproducible position of peaks independent of the channel in the chip where the measurements were taken, and independent of concentration of Herring DNA in solution. It is obvious, that even the minimal concentration of material 1 mg/ml, which is only 0.1%, is more than enough. Scaling with concentration enlarge is not observed. This fact probably means that all surface of a microfluidic channel already covered with attached bio-molecules from solution at this concentration. We

earlier observed in experiments that the first monolayer of bio-molecules near the interface with a substrate is the most important and gives strongest signature. The volume of material interrogated in these experiments is restricted by one channel of a chip with cross-section of 10 by 5 μm^2 on the length of 200 μm (opening of a microdetector) is at maximum 10^4 μm^3 or 10^{-8} ml. Thus, the amount of dry material at two concentrations was 0.01 ng (for concentration 1mg/ml) and 0.05 ng (for 5 mg/ml). The result indicates that even more diluted solutions are preferable for sample preparation. This will reduce the probability to clog the cannels and reduce all artificial effects in transmission spectra.

Averaged transmission spectra measured in three different channels is shown in Figure 5-4. The results clearly show that artifacts are smaller at concentration 1 mg/ml compare to 5 mg/ml. At the same time the results demonstrate a very good agreement in frequencies of resonance features for both concentrations. Although the overall pattern in the entire frequency range can be slightly different, the results of measurements in one channel are also good (Figure 5-5), having the same frequencies of the sharp transmission minima.

In the regions where transmission is greater than 1, the sharp transmission minima still observed and can be used for identification of absorption peak maxima (see the following section). It seems that the artifacts originate from differentiation of spectra at frequencies where transmission is equal to 1.

These experimental result already indicate extremely high sensitivity of spectrometer with microfluidic chips, thus promising the possibility of a single macromolecule and cell detection and identification.

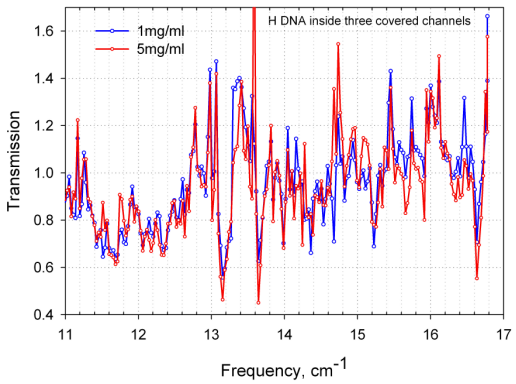

Figure 5-4. Averaged transmission of H DNA (two concentrations, 1mg/ml and 5 mg/ml, inside covered channels.

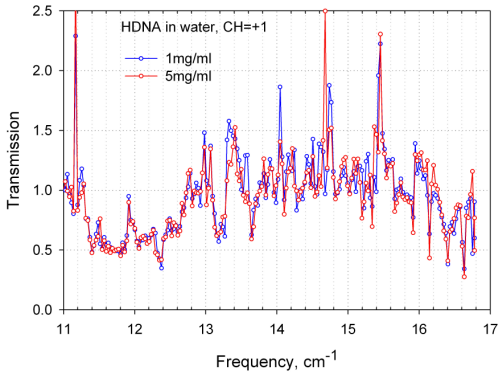

Figure 5-5. of H DNA two concentrations in the same channel.

Subtask 5.3. Theoretical analysis to calculate absorption coefficient spectrum from transmission measurements (consultant Prof. B. Gelmont).

The Maxwell- Garnett approximation is used for determination of the dielectric permittivity of biomaterial solution. The refractive index of the biomaterial is taken to be 1.65 according to our experimental data. A new approach to calculate transmission and absorption of biological materials in water or other solutions has provided new equations needed for data analysis.

We have found the dependence of the absorption coefficient on frequency from experimental dependence of the transmission using equations

$$\gamma = c\frac{\varepsilon_2 - \varepsilon_1}{2\varepsilon_1 + \varepsilon_2}, \qquad \varepsilon_{sol} = \varepsilon_1[1 + c\frac{3\gamma}{1-\gamma}],$$

where ε_1 is the dielectric permittivity of water, ε_2 is the dielectric permittivity of biomaterial, c is biomaterial concentration.

We have measured the ratio of the water and solution transmissions. The characteristics of water are known. So we can find the absorption coefficient of biomaterial. The corresponding code is written.

Figure 5-6 compares spectroscopic specific features in calculated extinction coefficient κ and transmission spectra.

Artifacts in the spectra of κ are revealed as sharp positive peaks at frequencies where T is changing from values below one values to above 1. Except these points, the frequencies of minima in transmission spectrum correlate well with the frequencies of maxima in extinction coefficient. This result is important indicating the analysis correctly identifies vibrational frequencies of bio-material in solutions using microfluidic devices, which are important for fingerprinting of bio-material.

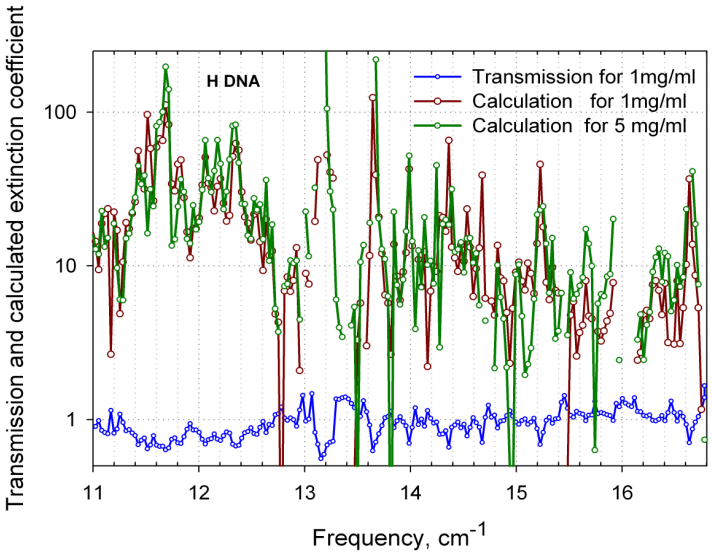

Figure 5-6. Calculated extinction coefficient κ and experimental transmission spectra of Herring DNA water solution.

CONCLUSIONS

A completely functioning nanofluidic sensor platform was developed, tested, and refined in combination with a THz spectroscopic system. The project was focused on further developments of an inexpensive nanofluidic technology toward future commercialization and fabrication. The efforts were aimed for stand-alone operation with sample injection and fluidic control built into the platform to facilitate transparent operation by the user. Micro/nanofluidic chips technology was developed, including a cover technology over the active area and integrating active region into total sample analysis chip. Instrumentation for automated flow control was developed and implemented. Interface packaging of fluidic platform with THz spectroscopic system was created. THz spectroscopic system was modified including: i) a new data acquisition system and software using National Instrument multifunctional module; ii) a new fluidic chip holder designed, fabricated and assembled with a syringe pump driving mechanism; iii) control system to allow flow through a microfluidic sample analysis chip; iv) a new detector housing to be combined with a micro/nanofluidic platform; v) an automated height positioning of the probe. The completed system was tested and evaluated. A new protocol was developed for spectroscopic characterization of biomaterials using nanofluidics. Spectroscopic characterization of biological materials in solutions was performed. Theory was developed to analyze

experimental data and to calculate absorption coefficient spectrum from transmission measurements in nanofluidics. Experimental characterization of sub-THz transmission spectra from DNA solution using microfluyidics demonstrated extremely high sensitivity of spectrometer with microfluidic chips in sub-THz range that required less than 0.01 ng of dry material. from solution with concentration less than 0.1 %.

References

1. HILL, N. E., 1963, *Trans. Faraday* Soc., 59,344-6.
2. Choy, T. C. Effective medium theory: principle and applications;
Clarendon Press: Oxford, 1999